electronics

MDPI

Article

Impact of the Exciter and Governor Parameters on Forced Oscillations

Naga Lakshmi Thotakura [1,*], Christopher Ray Burge [2] and Yilu Liu [1,3]

[1] Department of Electrical Engineering and Computer Science, The University of Tennessee, Knoxville, TN 37996, USA; liu@utk.edu
[2] Tennessee Valley Authority, Knoxville, TN 37902, USA
[3] Oak Ridge National Laboratory, Oak Ridge, TN 37830, USA
* Correspondence: nthotak1@vols.utk.edu

Abstract: In recent years, the frequency of forced oscillation events due to control system malfunctions or improper parameter settings has increased. Tuning the parameters of exciters and governor models is crucial for maintaining power system stability. Traditional simulation studies typically involve small transient disturbances or step changes to find optimal parameter sets, but existing optimization algorithms often fall short in fine-tuning for forced oscillations. Identifying the sensitive parameters within these control models is essential for ensuring stability during large, sustained disturbances. This study focuses on identifying these critical exciter and governor model parameters by analyzing their influence on sustained forced oscillations. Using Kundur's two-area system, we analyze common exciter models such as SCRX, ESST1A, and AC7B, along with governor models like GAST, HYGOV, and GGOV1, utilizing PSS®E software version 34. Sustained forced oscillations are injected at generator-1 of area-1, with individual parameter changes dynamically simulated. By considering a local oscillation frequency of 1.4 Hz and an inter-area oscillation mode of 0.25 Hz, we analyze the impact of each parameter change on the magnitude and frequency of forced oscillations as well as on active and reactive power outputs. This novel approach highlights the most influential parameters of each tested model—such as exciter, governor, and turbine gains, as well as time constant parameters—on the impact of forced oscillations. Based on our findings, the sensitive parameters of each tested model are ranked. These would provide valuable insights for industry operators to fine-tune control settings during oscillation events, ultimately enhancing system stability.

Keywords: exciter; governor; forced oscillation; SCRX; ESST1A; AC7B; GAST; GGOV1; HYGOV

Citation: Thotakura, N.L.; Burge, C.R.; Liu, Y. Impact of the Exciter and Governor Parameters on Forced Oscillations. *Electronics* **2024**, *13*, 3177. https://doi.org/10.3390/electronics13163177

Academic Editor: Spyridon Nikolaidis

Received: 23 June 2024
Revised: 4 August 2024
Accepted: 9 August 2024
Published: 11 August 2024

1. Introduction

The physical power system is divided into mechanical and electrical subsystems, as shown in Figure 1 [1]. The mechanical subsystem includes handling the fuel source, furnace, boiler, and turbine to generate and control steam flow. Using the fuel source, the furnace and boiler produce high-pressure steam, which the turbine converts into mechanical energy to drive the synchronous generator. The generator then converts this energy into electrical power. The governor control system regulates the generator's speed using droop speed control, adjusting the fuel supply based on grid frequency. An exciter, a type of DC generator, controls the field voltage (Efd) and current (Ifd) by supplying DC current to the generator's field winding to maintain a constant system voltage [2]. Exciters typically include an excitation power unit, excitation regulator, automatic voltage regulator (AVR), and power system stabilizer (PSS). The excitation power unit provides current to the generator rotor, while the excitation regulator adjusts the output. The AVR and PSS enhance system stability during disturbances [2].

For a generator exciter, certain parameters like limits, exciter time constant, voltage sensing time constant, and saturation value are fixed by the manufacturer. However, voltage regulator gains, time constants, reactive compensation, and limit level values are

tunable by the operator. Similarly, in the governor control system, parameters like water starting time, no-load gate, full load gate, turbine power fractions, maximum power, dead band, and turbine damping are fixed in the design, while droop, time constant, gains, and rate limits are tunable by the plant operator [3].

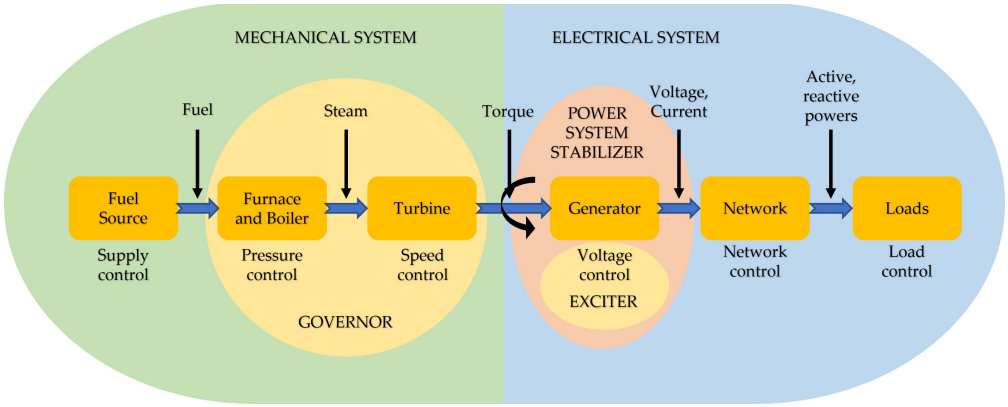

Figure 1. Block diagram of dynamic models in the physical power system structure.

Before commissioning a new unit into the grid, power system planning and operational studies analyze the grid's stability and reliability with the changes. These studies use detailed models of synchronous machines and their control systems to simulate real-world performance [3]. Sometimes, hardware-in-the-loop simulations are used to model and pre-tune synchronous generator controls [4]. During commissioning, extensive testing, including off-line, open-circuit, and online tests, tunes the governor and exciter parameters to ensure optimal performance and stability. Once set, these parameters maintain stable operation under various conditions, minimizing the need for frequent adjustments. Real-time manual adjustments to governor or exciter parameters are rare, typically occurring only in response to system disturbances or significant operational changes, with re-tuning performed during scheduled maintenance. However, specific oscillation events like low-frequency forced oscillations in nuclear or steam power plants require immediate attention for modal analysis and parameter fine-tuning.

Forced oscillations in power systems are typically triggered by external periodic disturbances from cyclic loads, equipment malfunctions, inadequate control design or parameter settings, mechanical oscillations of a generator under unusual conditions, or adverse interactions within the power system [5,6]. Growing forced oscillations within the low-frequency oscillations (LFO) or ultra-low-frequency oscillations (ULFO) range are increasingly serious and can damage equipment, restrict the ability to transfer power, and degrade the power quality. Additionally, resonance of a forced oscillation with weakly damped local or inter-area system modes can also result in high-magnitude oscillations. [7]. There have been numerous forced oscillation events that lasted for minutes to hours that have occurred around the world [8]. On 11 January 2019, the U.S. Eastern Interconnection experienced a forced oscillation event as a result of a defective input to a generator's steam turbine controller. The forced oscillation occurred for 18 min at a frequency of 0.25 Hz [9]. Bonneville Power Administration (BPA) reports several sustained oscillations due to interactions between the PSS and under-excitation limiter (UEL) of a hydropower plant. Also in 2016, active power erratic behavior was noticed due to problems with the interaction between a plant controller and the governor of a generating unit [10]. Several oscillation events across the U.S. summarizing generator equipment failures and the improper setting of system components like the governor, PSS, exciter, etc. rather than inaccurate modeling are discussed in [11,12]. Detecting and identifying the source of forced oscillations within the sub-control level of a generator remains an unsolved problem. However, analyzing oscillation trends and adjusting sub-control system parameters are crucial to restoring system stability in a short timeframe.

In the literature, several studies focus on tuning the AVR and PSS of the excitation system, using online tuning algorithms to adjust gain and time constant parameters to maintain system stability in real time [13–20]. However, the obtained parameters are acceptable for steady-state and small transient disturbance events and sometimes require an engineer's judgement for a few cases such as the wrong value of AVR gain, incorrect values of the PSS, bad turbine-governor data, wrong generator inertia and time constants, etc. [21]. These optimization algorithms are not suitable for tuning parameters during sustained forced oscillation events. Also, the level of accuracy of the algorithms depends on the field measurement transducers, which might not be available in all locations or may have inaccuracies. The authors of [22] studied the influence of excitation system PID control parameters of the power system using 5% step response dynamic characteristics. This study's results showed the parameters' impact on the transient response of the power system. In [23], the fault analysis was performed to find the root causes of the rectifier bridge filter and the excitation system's 24 V power supply failure causing two downtime accidents. These failures require a deep investigation of component analysis. But few oscillation events, which appear due to dynamic control model parameter inconsistencies in nuclear or steam plants, need immediate oscillation event re-creation and model parameters' re-tuning. However, in the literature, less attention was drawn towards the exciter parameters' tuning during large, forced oscillation events.

Similarly, most studies focus on tuning the PID parameters of a few governor models. Recent works [24–28] summarize the latest optimal algorithms for PID controllers for a hydro-turbine-based governor control. The importance of hydro power plant controller settings for suppressing frequency oscillations in the Turkish power system is highlighted in [29]. In [30], the authors discuss optimal techniques for tuning diesel governor parameters in hybrid renewable power systems using an exhaustive search approach. However, the tuning governor parameters described in [29,30] are for islanded mode operations. In [31], low-frequency oscillation events related to governor control are presented, including a special case scenario that analyzes how governor control parameters influence the damping characteristics of inter-area oscillations and introduce a special ultra-low-frequency model into the power system. A few case studies in [32–34] examined the impact of hydro-turbine and governor parameters on power systems with low- and ultra-low- frequency oscillations, focusing on isolated grid and single machine infinite bus system analyses. The work in [35] discusses the impact of governor and hydraulic model parameters on grid stability through eigenvalue analysis but does not address the influence of model parameters during fault and low-frequency oscillation scenarios.

The literature shows a scarcity of research on the impact of exciter and governor parameters on persistent forced oscillations. Few historical low-frequency oscillation events related to governor control have been studied, but there is limited focus on exciter parameters and their relation to oscillations. Moreover, the literature focuses on optimizing a few parameters of the control system all at a time for a new steady-state and/or small transient disturbance. The novelty of this paper lies in bridging this gap by analyzing how changes in tuning for each single governor and exciter parameter will affect the persisting forced oscillations on the system. The findings will equip power plant operators and planning engineers with the knowledge to adjust control system parameters effectively.

The major contributions of this paper are summarized as follows. It (1) considers the influence of tuning each excitor and governor model parameter one at a time on the forced oscillations for an oscillation frequency in the 0.25 Hz and 1.4 Hz modes using a PSS/E dynamic simulation, (2) identifies and ranks the most sensitive model parameters of the SCRX, ESST1A, and AC7B excitors models, (3) obtains and ranks the sensitive parameters of HYGOV, GAST, and GGOV1 models, and (4) examines the time domain and frequency domain analysis of the model parameters.

The rest of the paper is organized as follows: the process of forced oscillation injection and oscillation frequency modes are specified in Section 2; chosen exciter models, their standard parameters, and their tested range are described in Section 3 and Appendix A;

selected governor models and their parameters are specified in Section 4 and Appendix B; the simulation results of sensitive excitor and governor model parameters are discussed in Section 5; and the conclusions of the study are drawn in Section 6.

2. Methodology

This study was conducted on Kundur's two-area multi-machine system using PSS/E dynamic simulation tools. The system's schematic diagram and default synchronous machine models are shown in Figure 2 and Table 1, respectively.

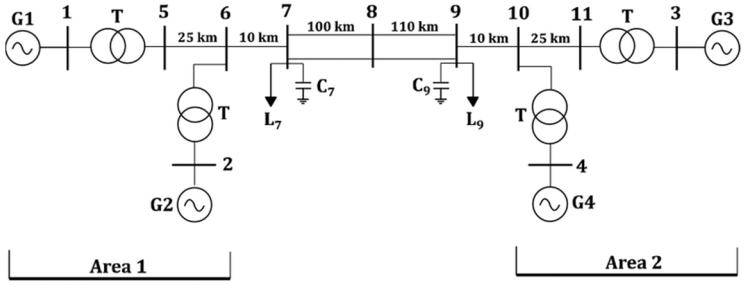

Figure 2. Schematic diagram of Kundur's two-area system. Reprinted from [16].

Table 1. Default models of Kundur's system.

Generator No.	Machine	Exciter	Governor	PSS
Gen-1, Gen-2, Gen-3, Gen-4	GENROE	ESST1A	TGOV1	IEEEST

The literature indicates that forced oscillation events associated with the governor control system typically occur at frequencies ranging from 0.1 to 0.38 Hz, with most at 0.25 Hz involving inter-area oscillations. Forced oscillation events caused by the exciter, AVR, and PSS generally range between 1 to 1.8 Hz, with most at 1.4 Hz involving local oscillations. To address both inter-area and local oscillation frequencies, this study selected oscillation frequencies of 0.25 Hz and 1.4 Hz. In this study, the forced oscillations were injected at the Gen-1 of Kundur's system using a sinusoidal signal with a fixed frequency introduced to the governor model's reference setpoint (G_{REF}) or the exciter model's voltage reference setpoint (V_{REF}) [2] as defined by:

$$\Delta P(t) = A * \sin(2\pi ft) \quad (1)$$

where 'f' is the selected frequency of the forced oscillation (0.25 Hz or 1.4 Hz), 'A' is the sinusoidal wave amplitude, and 'P(t)' is the active power added to the governor reference setpoint. There were 10 MW peak-to-peak active power oscillations injected into the governor models and 10 MVAR peak-to-peak reactive power oscillations injected into the exciter models starting from 2 s. The forced oscillation disturbance magnitude and frequency were maintained constant. At 2 s, each tunable exciter or governor parameter was individually changed in the dynamic simulation to study its impact on forced oscillations. The impact on the frequency, voltage response, exciter/governor output, and active/reactive power output responses of Gen-1 were recorded as outputs. For the exciter models, analyses on the frequency, voltage, and reactive power changes were performed to study the influence of exciter parameter change. Similarly, for the governor model, frequency and active power responses were analyzed to study the influence of governor parameters. The sensitive parameters of the tested models were identified and ranked accordingly. In this study, fast Fourier transform (FFT) was used to analyze and to identify the parameter change influence on the dominant frequency as well as the magnitude. The frequency data were sampled at a frequency of 120 Hz. For both the oscillation modes, the changes in the oscillation magnitude were plotted with respect to the parameter changes. The key parameter values that changed the oscillation frequency were specified.

3. Exciter Models

Traditionally, low-frequency oscillations in power systems are thought to be primarily connected to the high gain and quick reactions of excitation systems [34]. The use of the appropriate excitation system model and parameters in the power system stability calculation has a significant impact on the calculation results. Excitation system parameters including the excitation time constant, the excitation system static gain, the PID time constant, the open circuit time constant of the generator excitation windings, and so on may affect the output during disturbance simulations of a generator [22]. As a result, it is critical to the plant operator to investigate the influence of important excitation system parameters on generator transient characteristics. To provide a foundation for the identification, verification, and optimization of generator excitation parameters in real time, each of the model's selected exciter parameters were tested in this study.

A simple excitation control system called SCRX, a modified IEEE ST1A static excitation system, and an AC7B exciter model were selected to study their impact on the forced oscillations. The selected model block diagram, its associated parameters, and their tested parameters are specified in the following subsections. The ESST1A exciter of generator Gen-1 was replaced with the selected exciter model with the parameters specified in the respective tables. To study the parameters' impact, forced oscillations of magnitude 10 MVAR peak to peak with a frequency of 0.25 Hz and 1.4 Hz were injected into the V_{REF} of a selected exciter model. At 2 s, each of the individual exciter model parameters was varied within the specified range of the respective model (see table in Appendix A).

3.1. SCRX Exciter

The SCRX is a basic excitation system model that represents the generic properties of many different excitation systems. The block diagram of the SCRX excitation system is shown in Figure 3 [36]. The standard values of the model and the parameters tested range are given in Table A1 in Appendix A.

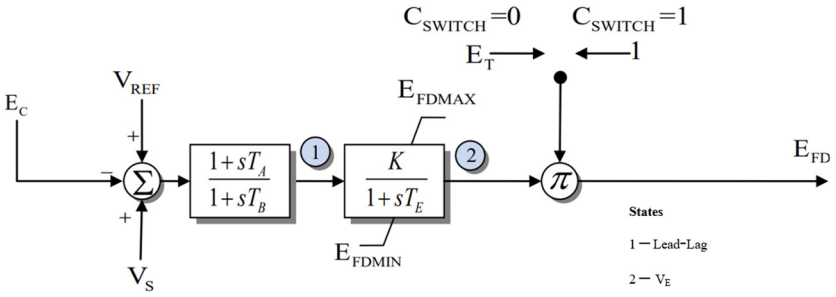

Figure 3. Block diagram of SCRX exciter model [36].

The voltage regulator reference voltage setpoint is denoted by V_{REF}. The input voltage (V_s)to the SCRX is obtained by adding three signals: the PSS signal (i.e., V_{OTHSG} signal), the under-excitation input limit (V_{UEL}), and the V_{OEL} signal (which is the difference between the reference voltage setpoint and the generator terminal voltage). E_C is the compensated terminal voltage. The tunable parameters in the SCRX exciter include the lead–lag block parameters T_A and T_B, exciter gain K, and time constant T_E parameters. The E_{FDMIN} and E_{FDMAX} parameters represent the minimum and maximum field voltage outputs. These parameters are tuned based on the steady-state and transient characteristics of the power system, which were studied in this model. C_{SWITCH} parameter distinguishes between systems (bus fed) in which the ac supply is proportional to the generator terminal bus voltage and systems (solid fed) in which the supply is independent of the generator terminal voltage. More details of the SCRX excitation system can be found in [37].

3.2. ESST1A Exciter

The ESST1A exciter is a modified IEEE ST1A static excitation system without an over-excitation limiter (V_{OEL}) and under-excitation limiter (V_{UEL}). The block diagram of ESST1A is shown below in Figure 4. The standard values of the model and the parameters tested range are given in Table A2 in Appendix A.

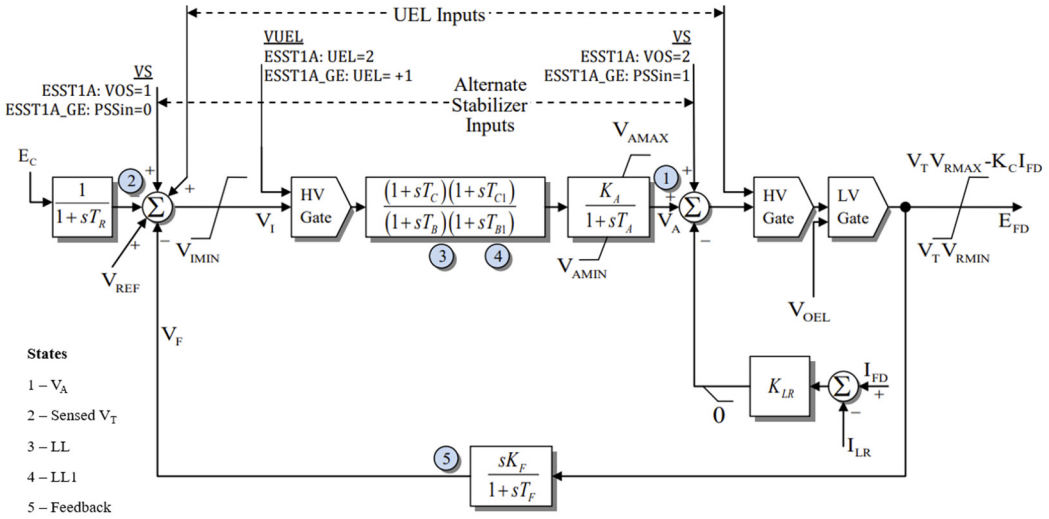

Figure 4. Block diagram of ESST1A exciter model [36].

Model ESST1A, a potential source-controlled rectifier-excitation system, is meant to simulate systems in which excitation power is provided from the generator terminals (or the unit's auxiliary bus) via a transformer and is regulated by a controlled rectifier. The maximum exciter voltage available from such systems is proportional to the voltage at the generator terminals [37]. Most of the ESST1A models employ fully controlled bridges. The inherent exciter time constants in this sort of system are quite modest; hence, exciter stabilization is typically not necessary. On the other hand, it may be beneficial to lower the transient gain of such devices for various reasons. The model given is adaptable enough to reflect transient gain reduction applied either in the forward path via time constants, T_B and T_C (in which case K_F would generally be set to zero), or in the feedback path via an appropriate choice of rate feedback parameters, K_F and T_F [38]. The second lead–lag block's time constants, T_{C1} and T_{B1}, indicate a representation of transient gain increase, in which case T_{C1} would be larger than T_{B1}. K_A and T_A reflect the voltage regulator gain and exciter time constants [37].

The internal limiter following the summing junction can be ignored in many cases, but the field voltage limits, which are functions of both terminal voltage (except when the exciter is supplied from an auxiliary bus, which is not supplied from the generator terminals) and generator field current, must be modeled. It is feasible to describe the field voltage limitations as linear functions of the generator field current. Furthermore, for most transformer-fed systems, K_C is fairly small, allowing the term to be ignored in many studies. The ESST1A model simulates a field current limiter to safeguard the generator rotor and exciter from damage that might occasionally occur because of these systems' extremely high forcing capabilities. K_{LR} and an I_{LR} start setting serve as the limit's gain indicators [38].

3.3. AC7B Exciter

The AC7B exciter is applied to ac/dc rotating exciters. To create the required dc fields, this excitation system combines a stationary or rotating rectifier with an ac alternator. The AC7B model is the result of advancements to previous ac excitation systems, which simply replaced the controls while preserving the ac alternator and diode rectifier bridge. Some of the characteristics of this excitation system are a quick exciter current limit (V_{FEMAX}) to

protect the ac alternator's field, a high bandwidth inner loop regulating generator field voltage or exciter current (V_A, K_{F1}, K_{F2}), and the PID generator voltage regulator (V_R). If the V_R lacks a derivative term, a separate rate feedback loop (K_{F3}, T_F) is used to stabilize it [38]. The block diagram and the parameters of the AC7B excitation system are shown in Figure 5 [36]. The notations, standard values, and the tested range of the AC7B model parameters are given in Table A3 in Appendix A.

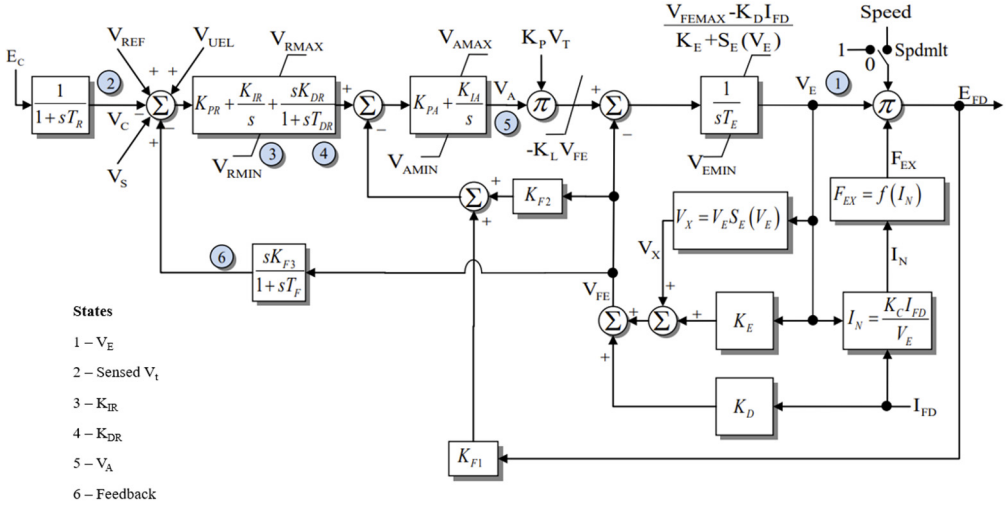

Figure 5. Block diagram of AC7B exciter model [36].

As shown in Figure 5, E_C is the compensated generator terminal voltage filtered through a filter block with a filter time constant denoted as T_R. The AC7B exciter consists of a regulator designed with PID control with proportional (K_{PR}), integral (K_{IR}), and derivative (K_{DR}) gains. The voltage regulator has proportional and integral gains represented as K_{PA}, K_{IA}, respectively. The brushless exciter is represented by T_E, K_E, S_E, K_C, and K_D parameters. The limits of V_E are used to represent the effects of a feedback limiter operation. This excitation system model includes the power source for the controlled rectifier. The user can set the logic switch to determine if the rectifier's power source is from terminal voltage (position "A") or independent of it (position "B"). More details about this model can be found in [38].

4. Parameters' Testing of Governor Models

The turbine-governor modeling is critical for transient rotor angle stability, frequency control, and, to a lesser extent, small-signal stability. A crucial component of the turbine-governor dynamics is fast-valving, which is the governor's quick response in the first couple of seconds after a grid disturbance. This control is distinguished by the quick closing of the intercept valves on a steam turbine in response to a nearby fault to reduce mechanical power on the generator shaft and, hence, limit shaft acceleration and the risk of rotor angle instability. Any such controls that will abruptly influence the mechanical output of the turbine as a result of a nearby grid fault must be modeled for transient stability studies [39]. An example is the installation of acceleration controls on gas turbines, which may be activated in some situations during a nearby catastrophic grid failure. However, acceleration controls are not available on all gas turbines. Also, where droop is implemented via electrical power feedback and the use of a proportional integral (PI) or proportional integral derivative (PID) controller in the turbine-governor controls can influence transient stability and should be modeled accordingly [39]. In the frequency range of electromechanical modes of rotor oscillation, the turbine governor may have a little negative dampening impact for small-signal stability concerns.

In this work, a simple gas turbine-governor model called GAST, a hydro-turbine-based HYGOV governor model, and a most used GGOV1 governor model were selected to study

their influence on forced oscillations. Each model block diagram, its associated parameters, and their tested parameters range are provided in the following subsections. The TGOV1 model of generator Gen-1 was replaced with the selected governor model with standard parameters. There were 10 MW peak-to-peak active power oscillations injected at the P_{REF} of the selected governor models. Each governor model parameters were changed one at a time to test their impact on the forced oscillations after 2 s. The parameters' change and their influence on the forced oscillations are discussed in the results section.

4.1. GAST Governor

This is the simplest basic illustration of a gas turbine. It assumes a simple droop control, a constant load limit (turbine rating), and three-time constants, one for the fuel valve response (T_1), one for the turbine response (T_2), and one for the load limit response (T_3). This model entirely disregards all aspects of a heavy-duty gas turbine's mechanics [17]. Figure 6 depicts the GAST gas turbine block diagram referred from PowerWorld [40].

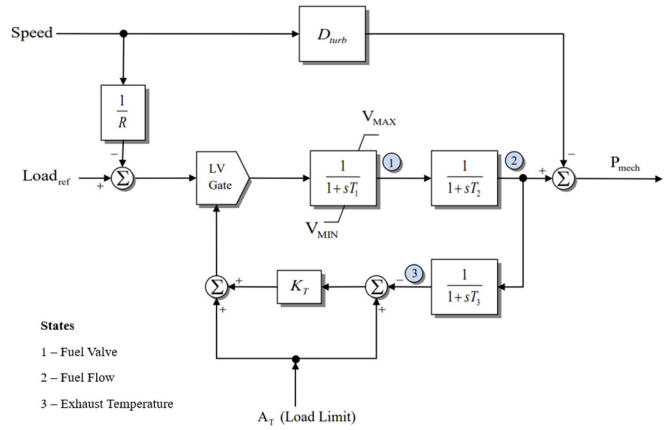

Figure 6. Block diagram of GAST governor model [38].

In the GAST model, the permanent droop is denoted by R. A_T denotes the ambient temperature load limit, and V_{MIN} and V_{MAX} are the minimum and maximum turbine power set limits. D_{turb} denotes the turbine damping factor. During commissioning of the unit, the speed governor parameters are obtained from gas injection setpoint change tests and load rejection tests, with damping factors and time constants tuned from load rejection; operational limits and permanent droop parameters are usually defined from steady-state tests [41]. In this work, the tunable parameters such as R, T1, T2, T3, K_T, D_{turb}, V_{MAX}, and V_{MIN} parameters were examined within the tested range specified in Table A4 in Appendix B.

4.2. HYGOV Governor

HYGOV is a basic non-linear hydroelectric-plant governor with a simple hydraulic representation of the penstock, unconstrained head, and tail race and no surge tank. Figure 7 shows the block diagram of the HYGOV governor model. The speed deviation from nominal to the actual speed (Δf) and the gate position (GV) in per unit are the inputs to the model, and P_{mech} is the output parameter. R and r are called the permanent and temporary droop parameters specified in per unit. The time constants of filter time constant (T_f), governor time constant (T_r), servo time constant (T_g), and water starting time constant (Tw) are the important parameters [42]. V_{elm} is the velocity limit, which is reciprocal to the time taken for the wicket gates to move from fully open to fully closed. H represents the per unit head. The qNL represents the no-load power flow rate required to maintain the rated speed while off-line. A_T is the turbine gain that tunes the turbine flow. D_{turb} is the turbine damping factor. These are the tunable parameters that can influence the performance of the

HYGOV during transient studies. Each of the individual parameters were tested to find the influence on the forced oscillations.

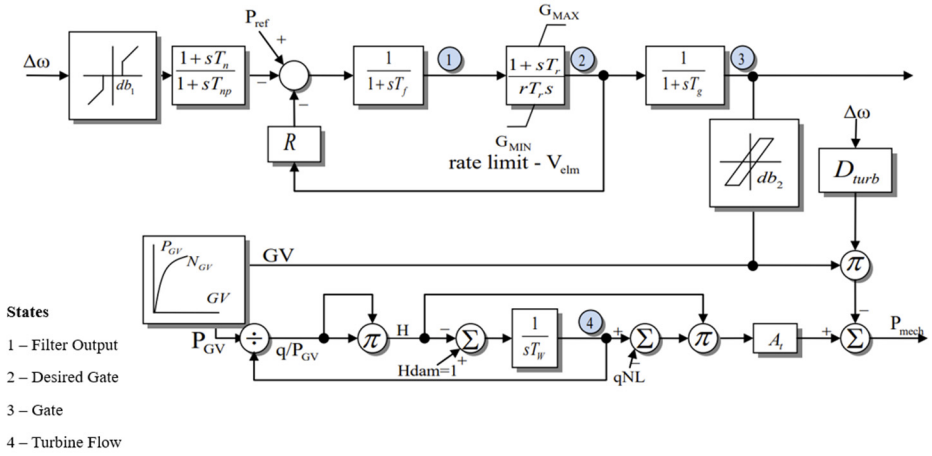

Figure 7. Block diagram of HYGOV governor model [38].

4.3. GGOV1 Governor

The GGOV1 model can be used to depict a wide range of prime movers that are controlled by PID governors and are often used in conjunction with a combustion turbine. Figure 8 shows the block diagram of the GGOV1 model. The notations of the model parameters, standard values, and the tested parameter range of the model are given in Table A6 in Appendix B.

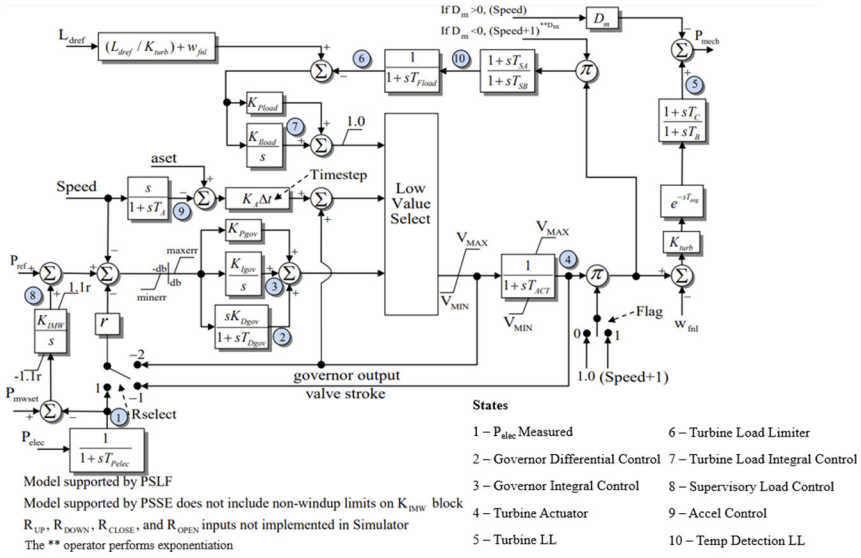

Figure 8. Block diagram of GGOV1 governor model [39].

Control blocks are also included in the model to simulate valve position and actuation, fuel system dynamics, a load limiter for exhaust temperature controls, a load controller for plant-level or outer loop controls, an acceleration limiter, and a governor deadband. More details about the modeling of the GGOV1 governor can be found in [43].

5. Results and Discussion

This section discusses the sensitive parameters of the selected exciter and governor models based on the influence of each parameter change on forced oscillations. For both the local oscillation frequency of 1.4 Hz and inter-area frequency of 0.25 Hz, the deviation of the forced oscillation magnitude, frequency response, change in active/reactive power

magnitude from the fixed frequency, and magnitude were used to rank the sensitive parameters. The analysis of individual parameter influence on the active power magnitude in governors and the reactive power characteristics in the exciter helped to understand and find the dominant parameters to see how each of these can alter the sustained forced oscillations. The parameters of the models were tested over a wide range to see if they have an impact on the forced oscillations and may cause instability in the system response or not. The specific results of each model are discussed in the respective subsections below.

5.1. SCRX Exciter

According to each parameter change, the impact on the forced oscillations' frequency, magnitude, reactive power output, the SCRX model parameters, and their respective ranks are shown in Table 2 below. Among the exciter models, the exciter gain was the most important parameter. The SCRX exciter gain (K) was changed from 10 to 1000 value, and the corresponding frequency and voltage responses are shown in Figure 9. The very low value of K = 10 caused instability in the system response. The value of K = 100 had around 10 MVAR of forced oscillation magnitude. Increasing the K value from 100 to 1000 in steps of 100 increased the oscillation magnitude of 10 MVAR to 21.436 MVAR and 86.422 MVAR for the 0.25 Hz and 1.4 Hz modes, respectively. Similarly, the gain reduction ratio (T_A/T_B) changed from 0.05 to 1.0 in steps of 0.1. The frequency and voltage responses of Gen-1 for the T_A/T_B change are shown in Figure 10.

Table 2. Sensitive parameters of SCRX exciter with respect to reactive power change.

SCRX Parameters	Tested Parameters' Range	Reactive Power Output (MVAR)		Rank
		0.25 Hz	1.4 Hz	
K—Exciter Gain	K—100	10.012	10.043	1
	K—1000	21.436	86.422	
T_A/T_B—Gain reduction ratio	T_A/T_B—0.1	10.044	10.051	2
	T_A/T_B—1.0	20.986	74.193	
T_E—Time constant	T_E—0.0	10.011	10.026	3
	T_E—1.0	0.601	0.859	
T_B—Time constant	T_B—1.0	15.697	9.962	4
	T_B—50.0	7.484	9.912	

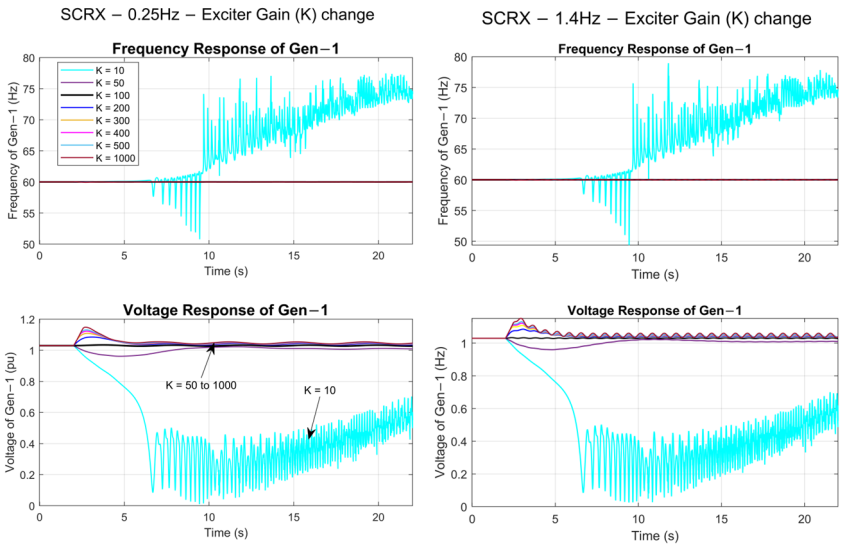

Figure 9. Response of SCRX exciter gain (K) changed from 10 to 1000 value in steps of 100.

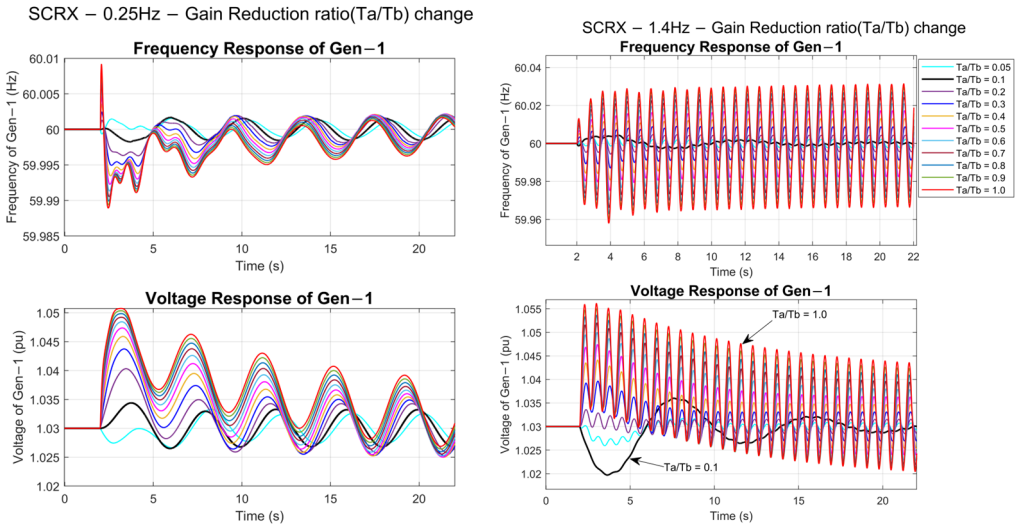

Figure 10. Response of gain reduction ratio (T_A/T_B) changing from 0.1 to 1.0 in steps of 0.1.

The increase in the T_A/T_B parameter value from 0.1 to 1.0 increased the oscillation magnitude to 20.986 MVAR and 74.193 MVAR for the 0.25 Hz and 1.4 Hz modes, respectively. In contrast, the time constants T_E and T_B values increased, reducing the oscillation magnitude for both oscillation modes, as shown in Table 2. The FFT analyses of the SCRX model parameters are shown in Figure 11. The increase in the K and T_A/T_B values increased the oscillation magnitude linearly for the 1.4 Hz local oscillation mode, and, for the low-frequency 0.25 Hz mode, a very small oscillation magnitude change was observed. The exciter time constant T_E significantly affected the system's dynamic response. At lower K values (K = 10, 50), the system's sensitivity to $T_E \geq 7$ was higher, resulting in a noticeable change in the oscillation frequency to 0.11719 Hz.

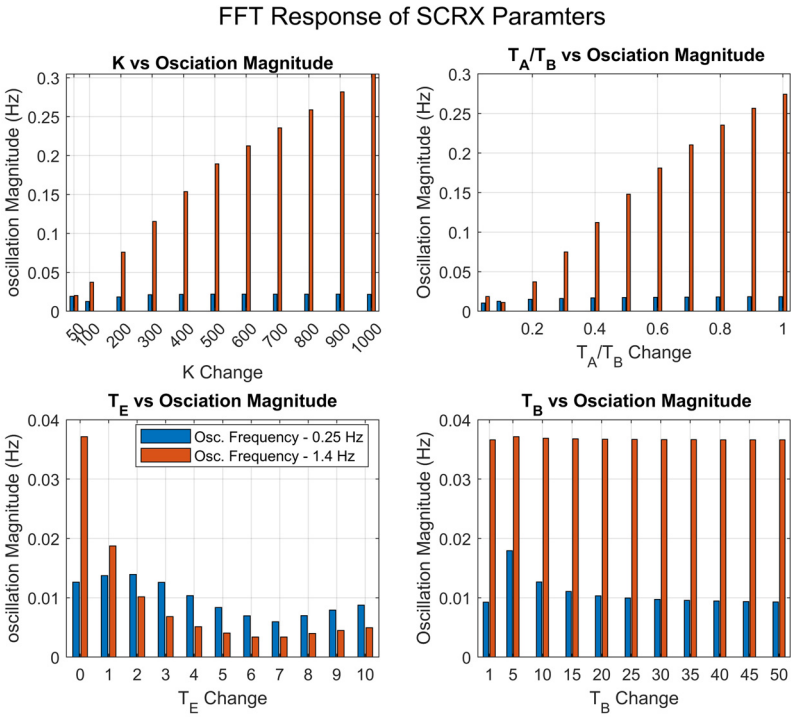

Figure 11. FFT response of the SCRX parameters.

5.2. ESST1A Exciter

The ESST1A exciter model plays a critical role in maintaining the stability of power systems by regulating voltage. To understand how changes in the ESST1A parameters influence forced oscillations, we conducted a comprehensive analysis by varying key parameters and measuring the resulting reactive power output (MVAR) at oscillation frequencies of 0.25 Hz and 1.4 Hz.

Our study focused on several parameters, including the voltage regulator gain (K_A), regulator time constant (T_A), voltage regulator time constant (T_C), filter time constant (T_R), and voltage regulator time constants (T_B and T_{B1}). The results, summarized in Table 3, indicated that changes in these parameters significantly impact the oscillation magnitudes and frequencies.

Table 3. Sensitive parameters of ESST1A exciter with respect to reactive power change.

ESST1A Parameters	Tested Parameters' Range	Reactive Power Output (MVAR)		Rank
		0.25 Hz	1.4 Hz	
K_A—Voltage regulator gain	K_A—50	0.32	0.5811	1
	K_A—1000	20.012	117.101	
T_A—Regulator time constant	T_A—0	10.022	10.041	2
	T_A—0.1 to 1	$T_A \geq 0.4$ induced growing oscillations with a frequency of 1.298 Hz		
T_C—Voltage regulator time constant	T_C—0	19.99	29.104	3
	T_C—1 to 10	Changed oscillation frequency to 13.33 Hz if $T_C > 6$		
T_R—Filter time constant	T_R—0	10.027	10.071	4
	T_R—1	24.316	24.154	
T_{B1}—Voltage regulator time constant	T_{B1}—0	26.918	117.118	5
	T_B—20	19.96	2.791	
T_B—Voltage regulator time constant	T_B—0	19.98	115.796	6
	T_B—20	17.554	45.229	
I_{LR}—Current limiter reference	$I_{LR} \leq 2$	System Unstable		
K_A —Voltage regulator gain	$K_A \leq 40$	System Unstable		
K_F —Excitation control system stabilizer gain	$K_F \geq 0.1$	System Unstable		
K_C—Rectifier loading factor	$K_C \geq 0.6$	System Unstable		
V_{AMAX} —Maximum voltage regulator output limit	$V_{AMAX} \leq 2$	System Unstable		
V_{AMIN}—Minimum voltage regulator output limit	$V_{AMIN} \geq 0.2$	System Unstable		
V_{RMAX}—Maximum voltage regulator output limit	$V_{RMAX} \leq 2$	System Unstable		
V_{RMIN}—Minimum voltage regulator output limit	$V_{RMIN} \geq 0.2$	System Unstable		
V_{IMAX}—Maximum voltage regulator input limit	$V_{IMAX} \leq 0$	System Unstable		
V_{IMIN}—Minimum voltage regulator input limit	$V_{IMIN} \geq 0.2$	System Unstable		

The voltage regulator gain (K_A) parameter was changed from 10 to 1000 in steps of 100. The low value of K = 50 had around a 0.5 MVAR forced oscillation magnitude. As shown in Table 3, increasing the exciter gain value from 50 to 1000 increased the oscillation magnitude to 20.012 MVAR and 117.101 MVAR for the 0.25 Hz and 1.4 Hz modes, respectively. The FFT response of K_A for the 1.4 Hz oscillation mode is shown in Figure 12. The low values of K_A from 50 to 400 showed a linear increase and, from 500 to 1000, the oscillation magnitude remained constant. Tuning extremely low values of KA $\leq$ 50 caused instability in the system. The regulator time constant (T_A) value was changed from 0 to 1 in steps of 0.1. As shown in Figure 13, for T_A values below 0.3 and above 0.5, the system appeared more stable with lower oscillation magnitudes. The middle range of T_A (0.3 to 0.5) led to higher oscillation magnitudes specifically for the 1.4 Hz mode, indicating potential instability with an oscillation frequency of 1.298 Hz in both modes.

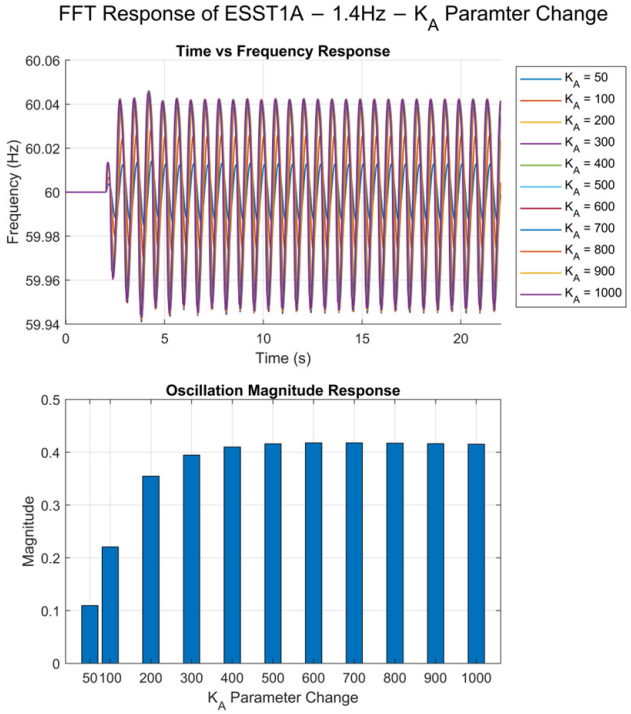

Figure 12. FFT response of the ESST1A model: K_A parameter change.

Similarly, the rise in the voltage regulator time constant (T_C) parameter value increased the oscillation magnitude to 110.137 MVAR. For both oscillation modes, the increase in $T_C > 8$ caused the change in oscillation frequency to 13.33 Hz. Likewise, the filter time constant (T_R) increased the forced oscillation magnitude from 10 MVAR to 24 MVAR with a T_R value increase from 0 to 1. In contrast, the increase in voltage regulator time constants T_B and T_{B1} values reduced the oscillation magnitude. As shown in Figure 13, the time constants T_A, T_C, T_R, T_B, T_{C1}, and T_{B1} had a large influence on the system stability for the 1.4 Hz mode. The ESST1A parameters K_{LR}, T_F, and T_{C1} showed no impact on the forced oscillations. The low values of the parameters $I_{LR} \leq 2$, $K_A \leq 40$, $V_{AMAX} \leq 2$, $V_{RMAX} \leq 2$, $V_{IMAX} \leq 0$, and $V_{REF} \leq 0.6$ can make the system became unstable. The higher values of these parameters $K_F \geq 0.1$, $K_C \geq 0.6$, $V_{AMIN} \geq 0.2$, $V_{RMIN} \geq 0.2$, and $V_{IMIN} \geq 0.2$ can also make the system become unstable. K_A, T_C, T_R, T_{B1}, and T_B were the sensitive parameters of the ESST1A exciter model.

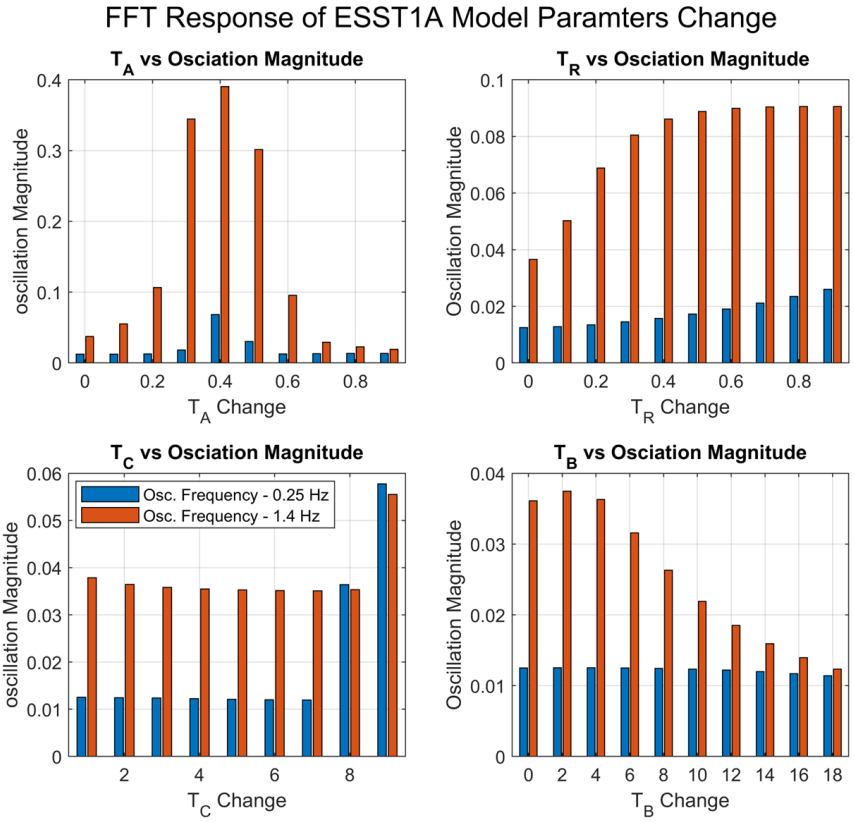

Figure 13. FFT response of the ESST1A model parameters.

5.3. AC7B Exciter

The sensitive parameters of the AC7B exciter model were identified based on the impact of the parameter change response on forced reactive power oscillations and were ranked, as shown in Table 4, as follows.

Table 4. AC7B exciter sensitive parameters and their associated ranks.

AC7B Parameters	Tested Parameters' Range	Reactive Power Output (MVAR)		Rank
		0.25 Hz	1.4 Hz	
K_{PA}—Voltage regulator proportional gain	K_{PA}—0 to 5	174.382	172.583	1
	K_{PA}—10 to 50	10	10	
K_E—Exciter constant related to self-excited field	K_E—0 to 0.2	67.716	75.955	2
	K_E—0.4–1.4	2.51	5.68	
	$K_E \geq 1.6$	System Unstable		
K_P—Potential circuit gain coefficient	K_P—0 to 5.0	10	10	3
	K_P—10 to 50	10	22.006	
K_{PR}—Regulator proportional gain	K_{PR}—0.0	28.671	0.992	4
	K_{PR}—50.0	10	18.709	
T_R—Regulator input filter time constant	T_R—0.0	10	10	5
	T_R—1.0	41.776	10	
V_{AMIN}—Regulator output minimum limit	$V_{AMIN} \leq -10.0$	22.032	23.884	6
	V_{AMIN}—0 to 40	10	10	

Table 4. *Cont.*

AC7B Parameters	Tested Parameters' Range	Reactive Power Output (MVAR)		Rank
		0.25 Hz	1.4 Hz	
K_{F1}—Excitation control system stabilizer gain	K_{F1}—0 to 0.5	10	10	7
	K_{F1}—1.0	6.181	3.721	
	$K_{F1} \geq 1.5$	System Unstable		
K_{F2}—Excitation control system stabilizer gain	K_{F2}—0	10	10	8
	K_{F2}—0.5 to 1.0	10	5.072	
	$K_{F2} \geq 2.5$	System Unstable		
K_{IR}—Regulator integral gain	K_{IR}—0 to 5.0	6.9658	8.0614	9
	K_{IR}—10 to 50	10	10	
K_{F3}—Excitation control system stabilizer gain	$K_{F3} \geq 1.5$	System Unstable		
T_E—Exciter time constant (>0)	$T_E \leq 0.3$	Distorted Oscillations		
V_{AMAX}—Maximum voltage regulator output limit	$V_{AMAX} \leq 0$	System Unstable		
V_{RMAX}—Maximum voltage regulator output limit	$V_{RMAX} \leq 2$	System Unstable		
VFE_{MAX}—Exciter field current limit reference	$VFE_{MAX} \leq 2$	System Unstable		

The voltage regulator gain (K_{PA}) parameter was changed from 0 to 50 in steps of 5.0, as shown in Figure 14. The low values of K_{PA} of 0 to 5 had around a 174 MVAR forced oscillation magnitude. Increasing the K_{PA} value from 10 to 50 maintained the oscillation magnitude to 10 MVAR for both oscillation frequency modes. For both the oscillation modes, the oscillation magnitude of the K_{PA}, K_{PR}, K_E, and T_R parameters from the FFT analysis is shown in Figure 15.

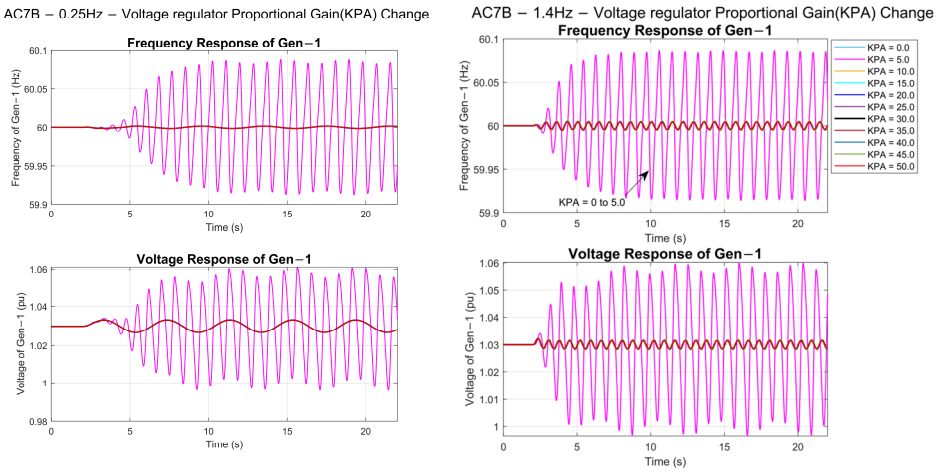

Figure 14. Response of voltage regulator proportional gain (K_{PA}) changing from 0.0 to 50.0.

Similarly, the rise in the excitor constant (K_E) parameter value from 0 to 1.4 decreased the oscillation magnitude to 2.51 MVAR and 5.68 MVAR for the 0.25 Hz and 1.4 Hz modes, respectively, as shown in Figure 15. In contrast, the increased values of the potential circuit gain coefficient (K_P), regulator proportional gain (K_{PR}), and filter time constant (T_R) increased the forced oscillation magnitude, as shown in Figure 15. The excitation control stabilizer gain K_{F1} oscillation magnitude response from the FFT analysis is shown in Figure 16. The K_{F1}, K_{F2}, and K_{F3} values between 0.5 to 1.0 had a stable response. The higher values of the parameters $K_E \geq 1.6$, $K_{F1} \geq 1.5$, $K_{F2} \geq 2.5$, and $K_{F3} \geq 1.5$ can cause the

system to become unstable. The lower values of $V_{AMAX} \leq 0$, $V_{RMAX} \leq 2$, and $VFE_{MAX} \leq 2$ can also make the system unstable. The AC7B exciter parameters Kc, K_{IR}, K_{DR}, K_{IA}, K_L, T_{DR}, T_{F3}, V_{EMIN}, V_{PSS}, E_1, E_2, $S(E_1)$, $S(E_2)$, V_R, and V_A did not show any influence on the forced oscillations. The regulator gains K_{PA}, K_{PR}, $K_{IR,}$ K_E, K_P, and T_R and the excitation control system stabilizer gains K_{F1} and K_{F2} were the sensitive parameters of the AC7B exciter model.

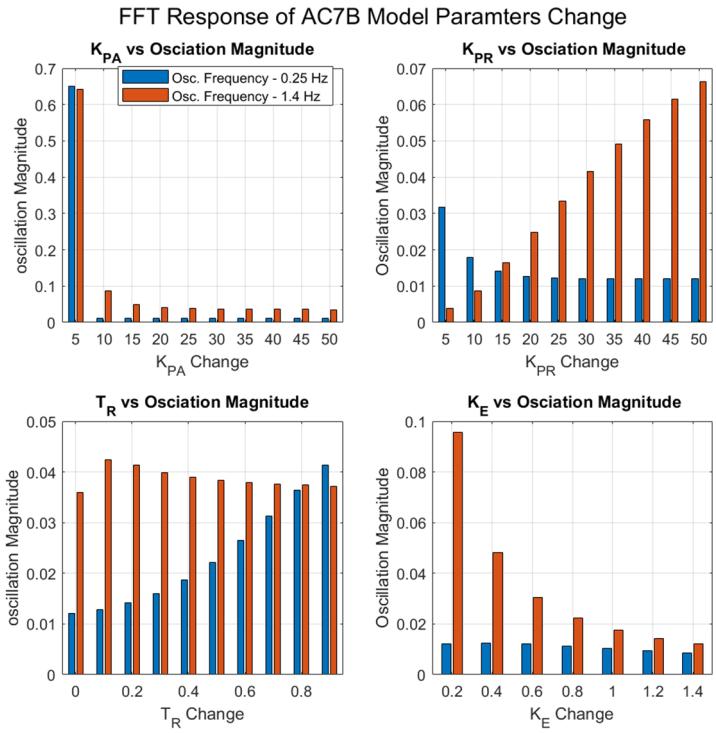

Figure 15. FFT response of AC7B model parameters.

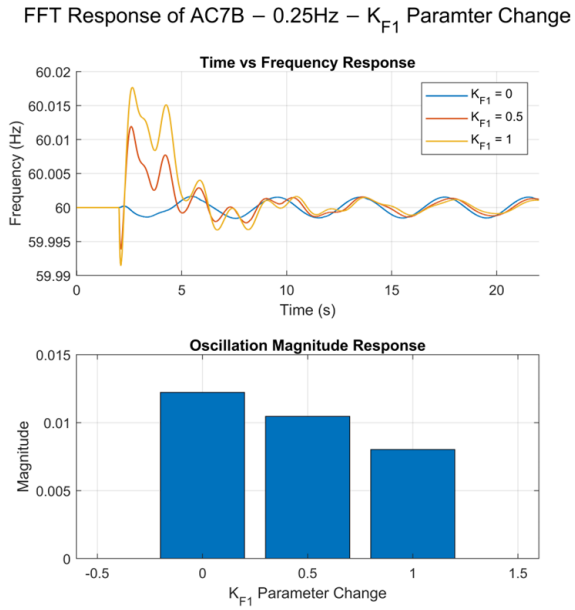

Figure 16. FFT response of excitation control system stabilizer gain K_{F1} change.

5.4. GAST Governor

The sensitivity of the GAST governor parameters was analyzed based on their influence on the forced oscillation magnitude, oscillation frequency, and active power oscilla-

tions of Gen-1. A forced oscillation magnitude of 10 MW peak to peak was applied at the GAST governor's P_{REF} input to assess these effects. The sensitive parameters of the GAST governor and their associated ranks are given in Table 5, as follows.

Table 5. GAST governor sensitive parameters and their associated ranks.

GAST Parameters	Tested Parameters Range	Active Power Output (MW)		Rank
		0.25 Hz	1.4 Hz	
R—Speed droop	R—0.0	Distorted oscillations		1
	R—0.1–1.0	13.339	10.089	
T_1—Governor mechanism time constant	T_1—0.0	16.917	10.091	2
	T_1—0.2 to 2.0	15.427	9.063	
T_2—Turbine power time constant	T_2—0.1	16.934	11.12	3
	T_2—2.1	13.038	10.026	
V_{MAX}—Maximum turbine power	V_{MAX}—0.0	19.8871	22.8798	4
	V_{MAX}—1 to 5	34.511	Damped oscillations	
V_{MIN}—Minimum turbine power	V_{MIN} = −4 to 1	34.791	Damped oscillations	5
	$V_{MIN} \geq 2$	Distorted oscillations	Distorted oscillations	

The speed droop (R) parameter was changed from 0 to 1. The low value of R = 0 had distorted oscillations with an oscillation frequency of 2.695 Hz for both oscillation frequency modes. As shown in Figure 17, increasing the speed droop value from 0.1 to 1 produced an oscillation magnitude of around 13.33 MW and 10.08 MW for the 0.25 Hz and 1.4 Hz modes, respectively. Likewise, the increase in time constants T_1 and T_2 values had a very small impact on the forced oscillation magnitude. However, the T_2 = 0 made the system become unstable. Its value should always be greater than 0, i.e., $T_2 \geq 0.1$. The minimum turbine power $V_{MIN} \geq 2$ made the system unstable. The graphs presented in Figure 18 show the FFT response of the GAST model parameters R, T_1, T_2, and T_3 changes. Each graph depicts the oscillation magnitude for two different oscillation frequencies, 0.25 Hz and 1.4 Hz, as the respective parameters were varied. Notably, the 0.25 Hz oscillations tended to exhibit higher magnitudes compared to the 1.4 Hz oscillations across all parameter changes.

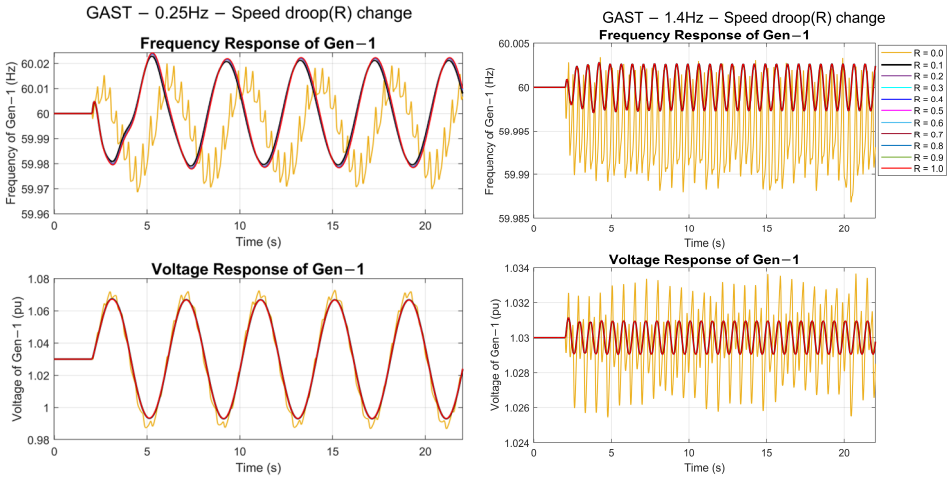

Figure 17. Response of speed droop (R) changing from 0.0 to 1.0 in steps of 0.1.

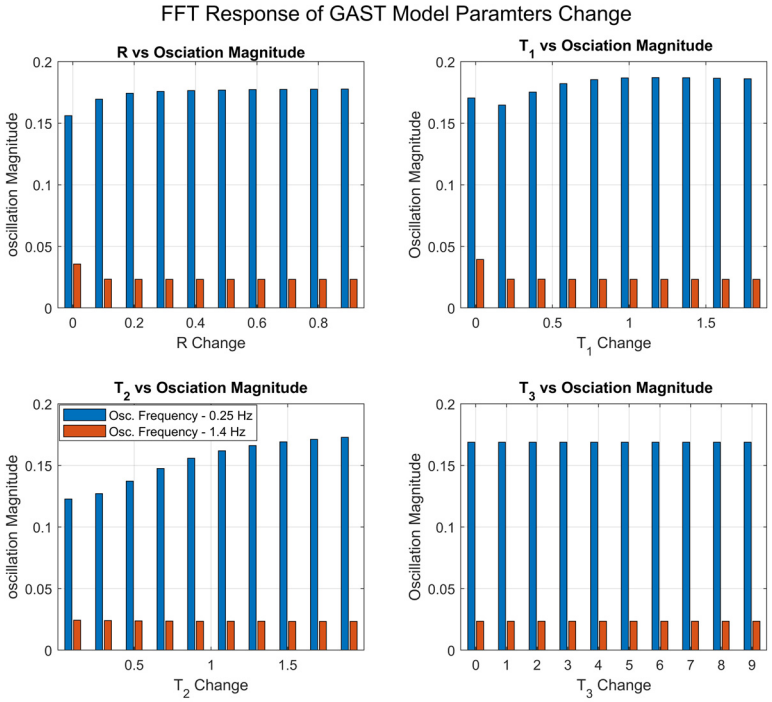

Figure 18. FFT response of GAST model parameters change.

The GAST parameters R, T_1, T_2, V_{MAX}, and V_{MIN} were the sensitive parameters of the model. The speed droop R = 0 and minimum turbine power $V_{MIN} \geq 2$ had distorted oscillations. The turbine damping factor (D_{turb}), temperature limiter gain (K_T), and the exhaust temperature time constant (T_3) of the GAST governor model did not show any influence on the forced oscillations.

5.5. HYGOV Governor

The sensitivity of the HYGOV governor parameters was analyzed based on their influence on the forced oscillation magnitude, oscillation frequency, and active power oscillations of Gen-1. The sensitive parameters of the HYGOV governor model were identified and ranked, as shown in Table 6, as follows.

Table 6. HYGOV governor model sensitive parameters and their associated ranks.

HYGOV Parameters	Tested Parameters' Range	Active Power Output (MW)		Rank
		0.25 Hz	1.4 Hz	
A_T—Turbine gain	A_T—−1 to 0; ≥1.5	System unstable; 390.33		1
	A_T—0 to 1	Damped oscillations		
r—Temporary droop	r—0.0	105.33	108.41	2
	r—0.2	25.47	9.8	
	r—2.0	2.9	5.709	
T_G—Servo time constant	T_G—0.1	11.188	21.832	3
	T_G—0.5	8.896	6.57	
	T_G—5.0	1.33	0.728	
T_W—Water time constant	T_W—0.0	8.046	5.674	4
	T_W—1.0	10.067	10.03	
	T_W—10.0	14.332	10.185	

Table 6. *Cont.*

HYGOV Parameters	Tested Parameters' Range	Active Power Output (MW)		Rank
		0.25 Hz	1.4 Hz	
T_R—Governor time constant	T_R—0	131.774	10.007	5
	T_R—5 to 50	10.097	10.012	
R—Permanent droop	R—0 to 0.2	10.05	10.13	6
	R—0.3 to 1.0	Damped oscillations	10.05	
Q_{NL}—No power flow	Q_{NL}—0 to 0.4	10.101	10.13	7
	Q_{NL}—0.45 to 0.5	10.066	Damped oscillations	
G_{MAX}—Maximum gate limit	$G_{MAX} \leq 0$	System unstable		
G_{MIN}—Maximum gate limit	$G_{MIN} \geq 2$	System unstable		

The turbine gain (A_T) was the most sensitive parameter of the HYGOV model. The A_T values, $A_T < 0$ and $A_T \geq 1.5$, made the system unstable and had around 390 MW oscillations. A_T values between 0 to 1 showed damped oscillations for both oscillation modes, as shown in Figure 19. The temporary droop (r) parameter was changed from 0 to 2, and the corresponding frequency and voltage responses are shown in Figure 20. The low value of r = 0 had high 105 MW oscillations for both frequency modes. Increasing the temporary droop value from 0.2 to 2 reduced the oscillation magnitude to 2.9 MW and 5.709 MW for the 0.25 Hz and 1.4 Hz modes, respectively.

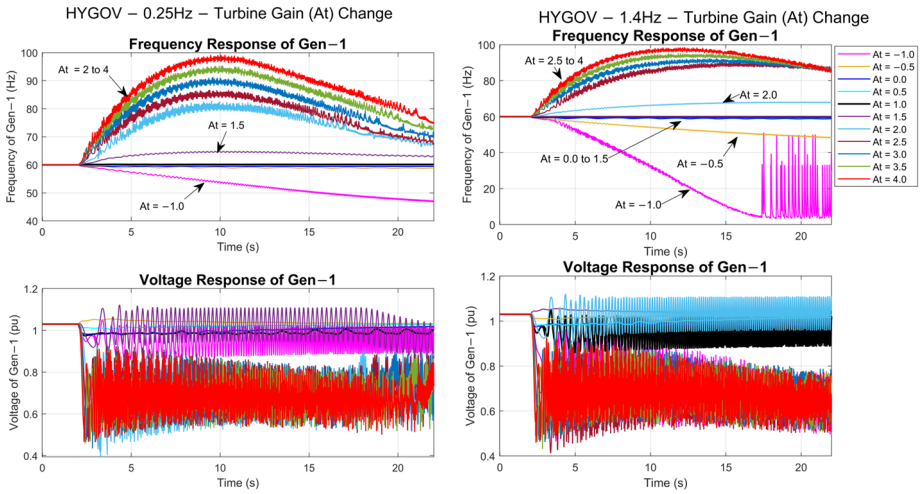

Figure 19. Response of turbine gain (A_T) changing from −1.0 to 4.0 in steps of 0.5.

Figure 21 presents the effect of varying four different parameters of the HYGOV model on the oscillation magnitude for two different oscillation frequencies (0.25 Hz and 1.4 Hz). Each subplot illustrates the oscillation magnitude in response to changes in specific parameters: R, temporary droop (r), T_G, and Tw. The speed droop R and T_G showed a significant increase in the oscillation magnitude as their values increased. Conversely, the temporary droop (r) parameter significantly reduced the oscillation magnitude with increasing values. The water inertia time constant (Tw) had a comparatively minor effect on the oscillation magnitude.

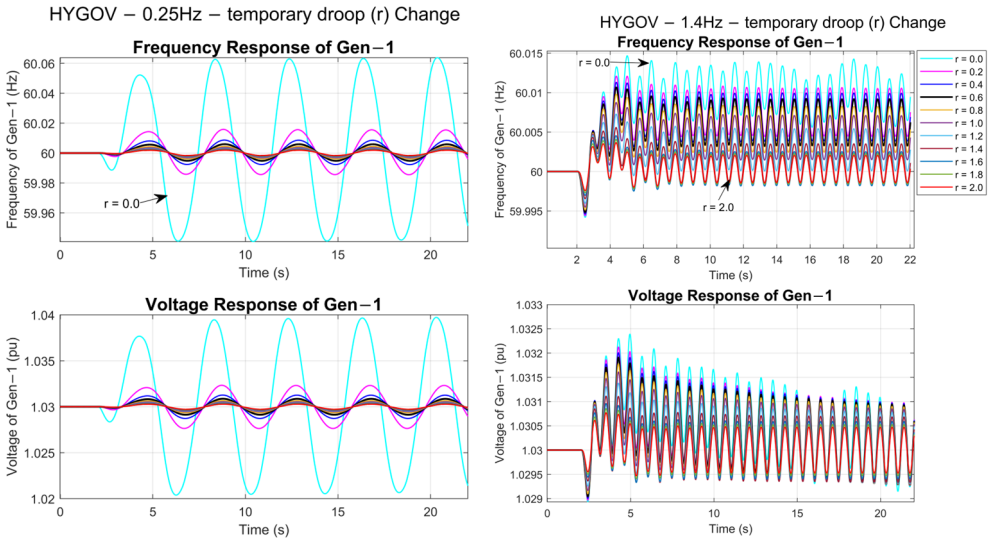

Figure 20. Response of temporary droop (r) changing from 0.0 to 2.0 in steps of 0.2.

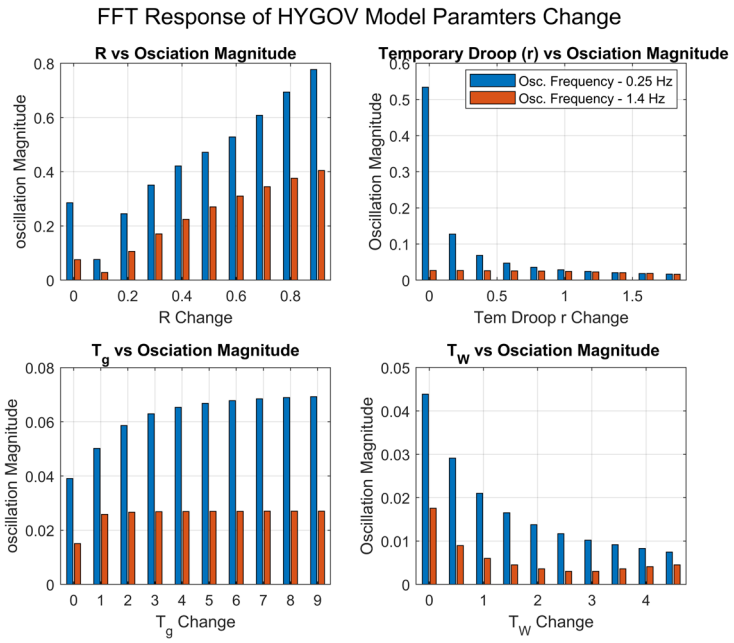

Figure 21. FFT response of HYGOV model parameters' change.

The higher values of permanent droop and no power flow had damped oscillations. The minimum and maximum gate limit values, $G_{MIN} \geq 2$ and $G_{MAX} \leq 0$, made the system unstable. The turbine gain was the most sensitive parameter, and $A_T < 0$ and $A_T > 1.5$ can make the system unstable. The permanent droop (R), temporary droop (r), servo time constant (T_G), and water time constant (T_W) were the sensitive parameters of the HYGOV model and had a more pronounced effect on the 0.25 Hz oscillation mode. Changing the maximum and minimum gate limits below or above these values of $G_{MAX} \leq 0$ and $G_{MIN} \geq 2$ can make the system become unstable.

5.6. GGOV1 Governor

The analysis focused on the sensitivity of various GGOV1 model parameters; specifically, their impacts on the reactive power output (MW) at two oscillation modes are discussed in this section. The parameters were ranked based on their influence on the system stability and oscillation magnitude, as summarized in Table 7.

Table 7. GGOV1 governor-sensitive parameters and their associated ranks.

GGOV1 Parameters	Tested Parameters' Range	Reactive Power Output (MW)		Rank
		0.25 Hz	1.4 Hz	
K_{turb}—Turbine gain	K_{turb}—0	Distorted oscillations—316.572		1
	K_{turb}—1	6.923	9.523	
	K_{turb}—2	10.876	14.739	
	K_{turb}—3	158.147	127.572	
	$K_{turb} \geq 4$	System unstable		
R—Permanent droop	R—0	Oscillations damped		2
	R—0.1	11.104	9.333	
	R—0.2	12.704	14.837	
	R—0.3 to 1.0	116.042	157.059	
T_C—Turbine lead time constant	T_C—0	10	10	3
	T_C—0.5	18.539	45.086	
	$T_C \geq 1$	System unstable		
W_{FNL}—No-load fuel flow	W_{FNL}—0.0	12.56	11.762	4
	W_{FNL}—0.4	6.292	8.89	
	W_{FNL}—0.6 to 0.8	Oscillations damped		
	W_{FNL}—1.0	System unstable—316.819		
T_{ACT}—Actuator time constant	T_{ACT}—0.0	9.997	48.295	5
	T_{ACT}—0.5	10.11	10.08	
	T_{ACT}—5.0	1.607	0.88	
T_B—Turbine lag time constant	T_B—0.1	10.21	10.324	6
	T_B—5.0	1.363	0.384	
K_{Pgov}—Governor proportional gain	K_{Pgov}—0	1.171	0.321	7
	K_{Pgov}—40.0	25.448	12.572	
K_{Igov}—Governor integral gain	K_{Igov}—0	9.292	7.542	8
	K_{Igov}—1 to 10	10.098	10.195	
K_A—Acceleration limiter gain	K_A—0	10.183	10.253	9
	K_A—20 to 50	10.012	12.57	
KI_{MW}—Power controller (reset) gain	KI_{MW}—1 to 10	Distorted oscillations		
V_{MAX}—Maximum valve position limit	$V_{MAX} \leq 0$	System unstable		
V_{MIN}—Minimum valve position limit	$V_{MIN} \geq 1.2$	System unstable		

The turbine gain (K_{turb}) was the most sensitive parameter of the GGOV1 model. The K_{turb} change response from 0 to 4 in steps of 1 is shown in Figure 22. The $K_{turb} < 0$ and Kturb ≥ 4 made the system unstable and had around 316 MW of oscillations. The K_{turb} values increasing from 1 to 3 increased the oscillation magnitude for both oscillation frequency modes. The permanent droop (R) parameter was changed from 0 to 1. The low value of R = 0 had damped oscillations for both frequency modes. Increasing the R value from 0.1 to 1 increased the oscillation magnitude to 116.04 MW and 157.059 MW for the 0.25 Hz and 1.4 Hz modes, respectively. The FFT response of R and actuator time constant (T_{ACT}) parameters are shown in Figure 23. The high values of T_{ACT} and turbine lag time constant (T_B) parameters also impacted the forced oscillation magnitude. In contrast, the increase in the governor proportional gain (K_{Pgov}) value increased the

oscillation magnitude. Likewise, the high values of the turbine lead time constant ($T_C \geq 1$) and no-load fuel flow ($W_{FNL} \geq 1$) can cause the system to become unstable.

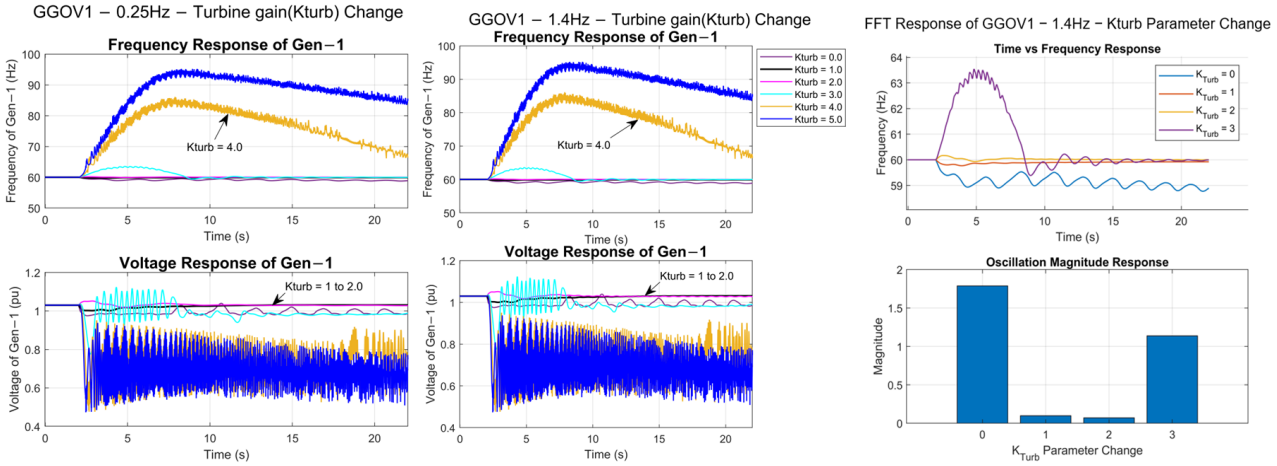

Figure 22. Time domain and FFT response of turbine gain (K_{turb}).

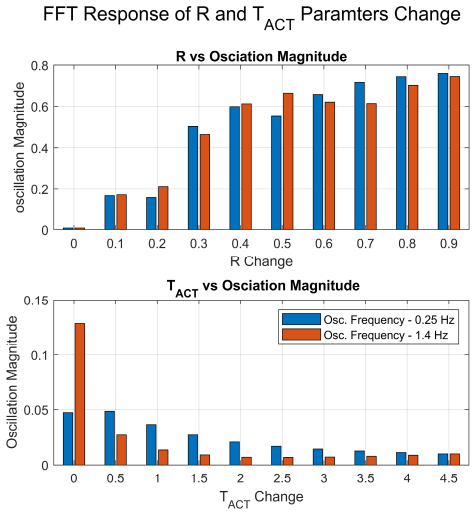

Figure 23. FFT response of R and T_{act} parameters' change.

The higher values of the parameters $V_{MIN} \geq 1.2$, $K_{turb} \geq 4$, $W_{FNL} \geq 1.0$, and $T_C \geq 1$ made the system unstable. The permanent droop $R > 0.1$, K_{Igov}, T_{Dgov}, T_{pelec}, and $L_{DREF} = 0$ delayed the system's response. The turbine gain (K_{turb}), permanent droop (R), turbine lead and lag time constants (T_C and T_B), actuator time constant (T_{ACT}), and no-load fuel flow (W_{FNL}) were the sensitive parameters of the GGOV1 governor model.

6. Conclusions

This study utilized Kundur's two-area system in PSS/E to investigate the impact of exciter and governor parameters on forced oscillations, presenting a comprehensive analysis that highlights the novelty of our approach. By examining widely used exciter models such as SCRX, ESST1A, and AC7B, alongside governor models like HYGOV, GAST, and GGOV1, we systematically injected forced oscillations and altered model parameters to assess their influence on frequency, voltage response, and oscillation magnitudes at 0.25 Hz and 1.4 Hz. This dual-frequency analysis encompasses both inter-area and local oscillation modes, providing a thorough understanding of parameter sensitivity.

The following key findings identify and rank the sensitive parameters of each model according to their impact on forced oscillations:

- **SCRX Model**: Parameters K, T_A/T_B, TE, and TB are the sensitive parameters of the SCRX exciter model. The oscillation magnitude for the 1.4 Hz mode increases linearly with K and T_A/T_B values, while the 0.25 Hz mode remains largely unaffected. The exciter time constant T_E significantly influences the oscillation frequency at lower values.
- **ESST1A Model**: Parameters K_A, T_C, T_R, T_{B1}, and T_B are highly sensitive, crucial for dynamic response and system stability. These parameters help to control forced oscillations. The parameters K_{LR}, T_F, and T_{C1} show no impact on the forced oscillations.
- **AC7B Model**: Sensitive parameters of this model include regulator proportional gains K_{PA}, K_{PR}, K_{IR}, K_E, K_P, T_R, $K_{F1,}$ and K_{F2}. Other parameters, such as Kc, K_{IR}, K_{DR}, K_{IA}, K_L, T_{DR}, T_{F3}, V_{EMIN}, E_1, E_2, $S(E_1)$, $S(E_2)$, V_R, and V_A, do not show any influence on the forced oscillations' stability.
- **GAST Model**: The speed droop parameter R significantly affects oscillation magnitudes and system stability. Parameters T_1, T_2, V_{MAX}, and V_{MIN} also influence oscillation characteristics.
- **HYGOV Model**: Sensitive parameters of this model include permanent droop R, temporary droop r, servo time constant T_G, and water time constant T_W, especially impacting the 0.25 Hz oscillation mode.
- **GGOV1 Model**: The most sensitive parameters are turbine gain K_{turb}, permanent droop R, turbine lead and lag time constants T_C and T_B, actuator time constant T_{ACT}, and no-load fuel flow W_{FNL}. The other parameters, R > 0.1, K_{Igov}, T_{Dgov}, and T_{pelec}, delayed the response of the system.

The ranking and identification of these sensitive parameters provides a novel approach to understanding and mitigating forced oscillations in power systems. This research offers practical insights for plant operators, enabling them to fine-tune control settings and improve system stability, thereby contributing to more resilient and reliable power system operations.

Author Contributions: Conceptualization, Y.L. and C.R.B.; methodology, N.L.T. and Y.L.; software, N.L.T. and Y.L.; validation, N.L.T., Y.L. and C.R.B.; formal analysis, N.L.T., Y.L. and C.R.B.; investigation, N.L.T. and Y.L.; resources, N.L.T.; data curation, N.L.T.; writing—original draft preparation, N.L.T.; writing—review and editing, N.L.T., Y.L. and C.R.B.; visualization, N.L.T. and Y.L.; supervision, Y.L. and C.R.B.; project administration, Y.L. and C.R.B.; funding acquisition, Y.L. All authors have read and agreed to the published version of the manuscript.

Funding: This work was supported by TVA via the CURENT industry partnership program and also made use of DOE AGM program funding.

Data Availability Statement: The original contributions presented in the study are included in the article, further inquiries can be directed to the corresponding author.

Conflicts of Interest: The authors declare no conflicts of interest.

Appendix A

The parameters of the tested SCRX, ESST1A, and AC7B exciter models, their standard values according to the NERC, PowerWorld, and PSSE documentation, and their tested parameter ranges for these models are specified in this section.

Table A1. Parameters of SCRX exciter model [36].

Name	Description	Parameters of Gen-1 SCRX Exciter	Parameter Range Tested
T_A/T_B	Gain reduction ratio	0.1	$0.05 < T_A/T_B < 1.0$
T_B	Time constant (s)	10.01	$1 < T_B < 50$
K	Exciter gain	100	$10 < K < 1000$

Table A1. *Cont.*

Name	Description	Parameters of Gen-1 SCRX Exciter	Parameter Range Tested
T_E	Time constant (s)	0.01	$0 \leq T_E < 1$
E_{MAX}	Maximum field voltage output (pu)	5	$2 < E_{MAX} < 10$
E_{MIN}	Minimum field voltage output (pu)	−4	$-5 < E_{MIN} \leq 0$
C_{SWITCH}	Voltage source switch Bus fed = 0, Solid fed = 1	0	C_{SWITCH} = 0 or 1
rc/rfd	Ratio of the crowbar resistance to the field winding resistance	0	$0 \leq$ rc/rfd ≤ 10
V_{REF}	Voltage regulator reference voltage (pu)	-	$0 < V_{REF} < 2.0$
V_S	Output voltage of a PSS (pu)	-	Off and ON
V_{UEL}	Under-excitation limiter		
V_{OEL}	Over-excitation limiter		
I_{FD}	Synchronous machine field current (pu)		

Table A2. Parameters of ESST1A exciter model [36].

Name	Description	Parameters of Gen-1 ESST1A Exciter	Parameter Range Tested
T_R	Filter time constant (s)	0.0167	$0 < T_R < 1$
V_{IMAX}	Maximum voltage regulator input limit	0.092	$0 < V_{IMAX} < 2$
V_{IMIN}	Minimum voltage regulator input limit	−0.083	$-1 < V_{IMIN} < 1$
T_C	Voltage regulator time constant (s)	1.2	$0 < T_C < 10$
T_B	Voltage regulator time constant (s)	2.5	$0 < T_B < 20$
T_{C1}	Voltage regulator time constant (s)	0	$0 < T_{C1} < 10$
T_{B1}	Voltage regulator time constant (s)	0	$0 < T_{B1} < 20$
K_A	Voltage regulator gain	600	$10 < K_A \leq 1000$
T_A	Voltage regulator time constant (s)	0	$0 \leq T_A < 1$
V_{AMAX}	Maximum voltage regulator output limit	4.14	$0 < V_{AMAX} < 10$
V_{AMIN}	Minimum voltage regulator output limit	−3.71	$-10 < V_{AMIN} < 0$
V_{RMAX}	Maximum voltage regulator output limit	4.14	$0 < V_{RMAX} < 10$
V_{RMIN}	Minimum voltage regulator output limit	−3.71	$-10 < V_{RMIN} < 0$
K_C	Rectifier loading factor proportional to commutating reactance (pu)	0.041	$0 < K_C < 0.6$
K_F	Excitation control system stabilizer gains (pu)	0	$0 < K_F < 1$
T_F	Excitation control system stabilizer time constant ($T_F > 0$) (s)	1	$0.1 < T_F < 2.1$
K_{LR}	Exciter output current limiter gain (pu)	18	$0 < K_{LR} < 50$
I_{LR}	Exciter output current limiter reference (pu)	3.953	$0 < I_{LR} < 10$

Table A3. Parameters of AC7B exciter model [36].

Name	Description	Parameters of Gen-1 AC7B Exciter	Parameter Range Tested
T_R	Regulator input filter time constant (s)	0.0167	$0.0 < T_R < 1$
K_{PR}	Regulator proportional gain (pu)	22.5	$0 < K_{PR} < 50$
K_{IR}	Regulator integral gain (pu)	22.5	$0 < K_{IR} < 50$
K_{DR}	Regulator derivative gain (pu)	0	$0 < K_{DR} < 40$
T_{DR}	Regulator derivative block lag time constant (s)	0	$0 < T_{DR} < 1$
V_{RMAX}	Regulator output maximum limit (pu)	4.52	$0 < V_{RMAX} < 10$
V_{RMIN}	Regulator output minimum limit (pu)	0	$-5 < V_{RMIN} < 5$
K_{PA}	Voltage regulator proportional gain (pu)	25	$0 < K_{PA} \leq 50$
K_{IA}	Voltage regulator integral gain (pu)	50	$0 < K_{IA} \leq 100$
V_{AMAX}	Regulator output maximum limit (pu)	31	$0 < V_{AMAX} < 50$
V_{AMIN}	Regulator output minimum limit (pu)	−31	$-10 < V_{AMIN} < 40$
K_P	Potential circuit gain coefficient (multiplier) (pu)	0	$0 < K_P < 50$
K_L	Exciter field voltage lower limit parameter (multiplier) (pu)	999	$0 < K_L < 20$
K_{F1}	Excitation control system stabilizer gain (pu)	0	$0 \leq K_{F1} < 5$
K_{F2}	Excitation control system stabilizer gain (pu)	1	$0 < K_{F2} \leq 5$
K_{F3}	Excitation control system stabilizer gain (pu)	0	$0 < K_{F3} \leq 5$
T_{F3}	Excitation control system stabilizer time constant (>0) (s)	1	$0.1 < T_{F3} \leq 2.1$
K_C	Rectifier loading factor proportional to commutating reactance (pu)	0	$0 < K_C \leq 1$
K_D	Demagnetizing factor, a function of AC exciter reactances (pu)	0.5	$0 < K_D \leq 2$
K_E	Exciter constant related to self-excited field (pu)	0.5	$0 < K_E \leq 2$
T_E	Exciter time constant (>0) integration rate associated with exciter control (s)	0.33	$0.1 < T_E \leq 2.1$
V_{FEMAX}	Exciter field current limit reference (> 0) (pu)	999	$0 < V_{FEMAX} < 10$
V_{EMIN}	Minimum exciter voltage output (pu)	0	$-5 < V_{EMIN} < 5$
E_1	Exciter alternator output voltages back of commutating reactance at which saturation is defined (pu)	3.51	$0 < E_1 \leq 10$
$S(E_1)$	Exciter saturation function value at the corresponding exciter voltage, E_1, back of commutating reactance (pu)	0.01	$0 < S(E_1) \leq 2$
E_2	Exciter alternator output voltages back of commutating reactance at which saturation is defined (pu)	4.68	$0 < E_2 \leq 10$
$S(E_2)$	Exciter saturation function value at the corresponding exciter voltage, E_2, back of commutating reactance (pu)	0.05	$0 < S(E_2) \leq 2$

Appendix B

Similarly, the parameters of the tested HYGOV, GAST, and GGOV1 governor models, their standard values according to the NERC, PowerWorld, and PSSE documentation, and their tested parameter ranges for these models are specified in this section.

Table A4. Parameters of GAST governor model [38].

Name	Description	Parameters of Gen-1—GAST Governor	Parameter Range Tested
R	Speed droop	0.05	$0 < R < 1$
T_1 (>0)	Governor mechanism time constant (s)	0.1	$0 < T_1 < 2$
T_2 (>0)	Turbine power time constant (s)	1.0	$0.1 < T_2 < 2.1$
T_3 (>0)	Turbine exhaust temperature time constant (s)	5.0	$0 < T_3 < 10$
A_T	Ambient temperature load limit	999.0	$0 < A_T < 10$
K_T	Temperature limiter gain	0.0	$0 < K_T < 10$
V_{MAX}	Maximum turbine power	1.0	$0 < V_{MAX} < 5$
V_{MIN}	Minimum turbine power	−0.05	$-4 < V_{MIN} < 2$
D_{turb}	Turbine damping factor	0.1	$0 < D_{turb} < 5$

Table A5. Parameters of HYGOV governor model [38].

Name	Description	Parameters of Gen-1 HYGOV Governor	Parameter Range Tested
R	Permanent droop (R < r)	0.07	$0 < R \leq 1$
r	Temporary droop	0.56	$0 < r \leq 2$
T_R (>0)	Governor time constant (s)	9.0	$0 < T_R \leq 50$
T_F (>0)	Filter time constant (s)	0.4	$0 < T_F \leq 0.5$
T_G (>0)	Servo time constant (s)	0.33	$0.1 < T_G \leq 5$
$\pm V_{ELM}$	Gate velocity limit	0.07	$0 < V_{ELM} \leq 1$
G_{MAX}	Maximum gate limit (GMIN < GMAX)	1.0	$0 < G_{MAX} \leq 10$
G_{MIN}	Minimum gate limit	0.0	$-5 \leq G_{MIN} < 5$
T_W (>0)	Water time constant	1.0	$0 < T_W < 10$
A_T	Turbine gain	1.25	$-1 < A_T < 4$
D_{turb}	Turbine damping	1.0	$0 \leq D_{turb} < 10$
q_{NL}	No power flow	0.07	$0 \leq q_{NL} < 0.5$

Table A6. Parameters of GGOV1 governor model [38].

Name	Description	Parameters of Gen-1 GGOV1 Governor	Tested Parameter Range
R	Permanent droop (pu)	0.04	$0 < R \leq 1$
T_{pelec}	Electrical power transducer time constant (s)	1.0	$0 < T_{pelec} \leq 10$
M_{AXERR}	Maximum value for a speed error signal	0.05	
M_{INERR}	Minimum value for a speed error signal	−0.05	
K_{Pgov}	Governor proportional gain	10	$0 < K_{Pgov} \leq 40$
K_{Igov}	Governor integral gain	2	$0 < K_{Igov} \leq 10$
K_{Dgov}	Governor derivative gain	0	$0 < K_{Dgov} \leq 10$
T_{Dgov}	Governor derivative controller time constant (s)	1	$0 < T_{Dgov} \leq 5$
V_{MAX}	Maximum valve position limit	1	$0 < V_{MAX} \leq 10$
V_{MIN}	Minimum valve position limit	0.15	$-2 \leq V_{MIN} < 2$

Table A6. *Cont.*

Name	Description	Parameters of Gen-1 GGOV1 Governor	Tested Parameter Range
T_{act}	Actuator time constant (s)	0.5	$0 < T_{act} \leq 5$
K_{turb}	Turbine gain	1.5	$0 < K_{turb} \leq 5$
W_{fnl}	No-load fuel flow (pu)	0.2	$0 < W_{fnl} \leq 1$
T_B	Turbine lag time constant (s)	0.1	$0.1 < T_B \leq 5$
T_C	Turbine lead time constant (s)	0	$0 < T_C \leq 2.5$
T_{eng}	Transport lag time constant for diesel engine (s)	0	$0 < T_{eng} \leq 5$
T_{fload}	Load limiter time constant (s)	3	$0 < T_{fload} \leq 10$
K_{pload}	Load limiter proportional gain for PI controller	2	$0 < K_{pload} \leq 10$
K_{Iload}	Load limiter integral gain for PI controller	0.67	$0 < K_{Iload} \leq 10$
L_{dref}	Load limiter reference value (pu)	1	$0 < L_{dref} \leq 10$
D_m	Mechanical damping coefficient (pu)	0	$0 < D_m \leq 10$
R_{open}	Maximum valve opening rate (pu/s)	0.1	
R_{close}	Maximum valve closing rate (pu/s)	−0.1	
KI_{mw}	Power controller (reset) gain	0	$0 < KI_{mw} \leq 10$
A_{SET}	Acceleration limiter setpoint (pu/s)	0.01	$0 < A_{SET} \leq 10$
K_A	Acceleration limiter gain	10	$0 < K_A \leq 50$
T_A	Acceleration limiter time constant (s)	0.1	$0 < T_A \leq 10$
T_{rate}	Turbine rating (MW)	800.0	
db	Speed governor deadband	0.0	$0 < db \leq 1$
T_{sa}	Temperature detection lead time constant (s)	4.0	$0 < T_{sa} \leq 10$
T_{sb}	Temperature detection lag time constant (s)	5.0	$0 < T_{sb} \leq 10$
R_{up}	Maximum rate of load limit increase	99	
R_{down}	Maximum rate of load limit decrease	−99	

References

1. Sauer, P.W.; Pai, M.A.; Chow, J.H. *Power System Dynamics and Stability: With Synchrophasor Measurement and Power System Toolbox*; John Wiley & Sons: Hoboken, NJ, USA, 2017.
2. Kundur, P.; Malik, O.P. *Power System Stability and Control*; McGraw-Hill Education: Cambridge, MA, USA, 2022; ISBN 9781260473544.
3. Hajagos, L.; Barton, J.; Berube, R.; Coultes, M.; Feltes, J.; Lanier, G.; Patterson, S.; Pereira, L.; Pourbeik, P.; Schneider, A.; et al. Guidelines for generator stability model validation testing. In Proceedings of the 2007 IEEE Power Engineering Society General Meeting, Tampa, FL, USA, 24–28 June 2007; pp. 1–16.
4. Mohammad, A.; Upreti, A. *Modeling and Pre-Tuning Governor and Exciter through Hardware-in-the-Loop Simulation*; Schweitzer Engineering Laboratories, Inc.: Washington, DC, USA, 2022.
5. Alshuaibi, K.; Zhao, Y.; Zhu, L.; Farantatos, E.; Ramasubramanian, D.; Yu, W.; Liu, Y.; Alshuaibi, K.; Zhao, Y.; Zhu, L.; et al. Forced Oscillation Grid Vulnerability Analysis and Mitigation Using Inverter-Based Resources: Texas Grid Case Study. *Energies* **2022**, *15*, 2819. [CrossRef]
6. Trudnowski, D.J.; Guttromson, R. A Strategy for Forced Oscillation Suppression. *IEEE Trans. Power Syst.* **2020**, *35*, 4699–4708. [CrossRef]
7. Zhi, Y.; Venkatasubramanian, V. Analysis of Energy Flow Method for Oscillation Source Location. *IEEE Trans. Power Syst.* **2021**, *36*, 1338–1349. [CrossRef]
8. Ghorbaniparvar, M. Survey on Forced Oscillations in Power System. *J. Mod. Power Syst. Clean Energy* **2017**, *5*, 671–682. [CrossRef]
9. Eastern Interconnection Oscillation Disturbance January 11, 2019, Forced Oscillation Event. 2019. Available online: https://www.nerc.com/pa/rrm/ea/Documents/January_11_Oscillation_Event_Report.pdf (accessed on 1 September 2022).

10. Kosterev, D.; Burns, J.; Leitschuh, N.; Anasis, J.; Donahoo, A.; Power, B.; Trudnowski, U.D.; Donnelly, M.; Pierre, J. Implementation and Operating Experience with Oscillation Detection Application at Bonneville Power Administration 2016 Grid of the Future Symposium. Available online: https://naspi.org/sites/default/files/2017-03/01_bpa_donnelly_NASPI_presentation.pdf (accessed on 20 November 2022).
11. Using Synchrophasor Data to Diagnose Equipment Health and Mis-Operations Event Summary Table Description. Available online: https://www.naspi.org/sites/default/files/reference_documents/13.pdf (accessed on 1 August 2022).
12. Silverstein, A. Diagnosing Equipment Health and Mis-Operations with PMU Data. 2015. Available online: https://www.naspi.org/sites/default/files/reference_documents/14.pdf (accessed on 1 August 2022).
13. Moshref, A.; Wooster, N.; Massey, N. Optimal Tuning of the Automatic Voltage Regulator-A General Approach. Available online: https://cigreconference.ca/papers/2022/paper_478.pdf (accessed on 3 April 2023).
14. Viveros, E.R.C.; Taranto, G.N.; Falcao, D.M. Tuning of generator excitation systems using meta-heuristics. In Proceedings of the 2006 IEEE Power Engineering Society General Meeting, Montreal, QC, Canada, 18–22 June 2006; p. 6.
15. Sambariya, D.K.; Nath, V. Optimal control of automatic generation with automatic voltage regulator using particle swarm optimization. *Univers. J. Control Autom.* **2015**, *3*, 63–71. [CrossRef]
16. Furat, M.; Cücü, G.G. Design, implementation, and optimization of sliding mode controller for automatic voltage regulator system. *IEEE Access* **2022**, *10*, 55650–55674. [CrossRef]
17. Sikander, A.; Thakur, P. A new control design strategy for automatic voltage regulator in power system. *ISA Trans.* **2020**, *100*, 235–243. [CrossRef] [PubMed]
18. Rais, M.C.; Dekhandji, F.Z.; Recioui, A.; Rechid, M.S.; Djedi, L. Comparative study of optimization techniques based pid tuning for automatic voltage regulator system. *Eng. Proc.* **2022**, *14*, 21. [CrossRef]
19. Tang, B.X. Parameter Tuning and Experimental Results of Power System Stabilizer. Master's Thesis, Louisiana State University and Agricultural and Mechanical College, Baton Rouge, LO, USA, 2011.
20. Abdel-Magid, Y.L.; Abido, M.A.; Mantaway, A.H. Robust tuning of power system stabilizers in multimachine power systems. *IEEE Trans. Power Syst.* **2000**, *15*, 735–740. [CrossRef]
21. Reliability Guideline, NERC, Power Plant Dynamic Model Verification Using PMUs. 2016. Available online: https://naspi.org/sites/default/files/2017-03/nerc_quint_power_plant_model_20160324.pdf (accessed on 3 November 2022).
22. Chen, Q.; He, J.; Huang, W.; Shu, X.; Li, W. Study on Influence of Excitation System Parameters on Transient Characteristics of Power Units. 2015. Available online: https://www.atlantis-press.com/article/25845095.pdf (accessed on 1 August 2022).
23. Zhu, Y.; Zhang, Y.; Xie, X. Analysis and Preventive Measures of Excitation System Failure Leading to Two Downtime Accidents. *IOP Conf. Ser. Earth Environ. Sci.* **2020**, *512*, 012171.
24. Niasse, M.; Zheng, Q.; Xin, A.; Quan, F.F.; Saleem, A.; Iqbal, A. Improved accuracy optimal tuning method for hydropower units' governor controller. *IOP Conf. Ser. Earth Environ. Sci.* **2020**, *508*, 012187. [CrossRef]
25. Andrade, J.G.P.; Júnior, E.L.; Ribeiro, L.C.L.J. Using genetic algorithm to define the governor parameters of a hydraulic turbine. *IOP Conf. Ser. Earth Environ. Sci.* **2010**, *12*, 012020. [CrossRef]
26. Singh, M.K.; Naresh, R.; Gupta, D.K. Optimal tuning of temporary droop governor of hydro power plant using genetic algorithm. In Proceedings of the 2013 International Conference on Energy Efficient Technologies for Sustainability, Nagercoil, India, 10–12 April 2013; pp. 1132–1137.
27. Perng, J.W.; Kuo, Y.C.; Lu, K.C. Design of the PID controller for hydro-turbines based on optimization algorithms. *Int. J. Control Autom. Syst.* **2020**, *18*, 1758–1770. [CrossRef]
28. Huang, Q.S.; Zhai, X.J.; Zheng, Y.; Xu, G.W.; Wang, H. Study on Stability of Hydroelectric Generating Set Influenced by the Governor Parameters under Isolated Grid. *Adv. Mat. Res.* **2014**, *875–877*, 1799–1803. [CrossRef]
29. Cebeci, M.E. The Effects of Hydro Power Plants' Governor Settings on the Turkish Power System Frequency. Master's Thesis, Middle East Technical University, Ankara, Turkey, 2008.
30. Asad, M.; Martinez, S.; Sanchez-Fernandez, J.A. Diesel Governor Tuning for Isolated Hybrid Power Systems. *Electronics* **2023**, *12*, 2487. [CrossRef]
31. Liu, Z.; Yao, W.; Wen, J.; Cheng, S. Effect analysis of generator governor system and its frequency mode on inter-area oscillations in power systems. *Int. J. Electr. Power Energy Syst.* **2018**, *96*, 1–10. [CrossRef]
32. Chen, L.; Lu, X.; Min, Y.; Zhang, Y.; Chen, Q.; Zhao, Y.; Ben, C. Optimization of governor parameters to prevent frequency oscillations in power systems. *IEEE Trans. Power Syst.* **2017**, *33*, 4466–4474. [CrossRef]
33. Hasan, A.; Wei, M.; Rui, X.; Zhu, W.; Yan, W.; Sun, Y.; Power, Q.X.; Bureau, S. Research on Governor Parameter Optimization to Suppress Ultra-Low Frequency Oscillation of Power System Caused by Hydropower Unit. *J. Phys. Conf. Ser.* **2021**, *9*, 2087.
34. Li, X.; Zhang, C.; Zhu, J.; Hu, X. The Effect of Hydro Turbines and Governors on Power System Low Frequency Oscillations. In Proceedings of the 2006 International Conference on Power System Technology, POWERCON2006, Chongqing, China, 22–26 October 2006.
35. Zangmo, G.; Om, K.; Uhlen, K. Impact of Hydro-Turbine and Governor Parameters on Stability of Grid Connected Power System. *Int. J. Electr. Eng. Inform.* **2017**, *9*, 1–12.
36. Block Diagrams, PowerWorld Corporation. Available online: https://www.powerworld.com/files/Block-Diagrams-17.pdf (accessed on 1 January 2024).

37. PSS®E 34.9.6, Program Application Guide Volume 2, August 2023, Siemens Industry, Inc. Siemens Power Technologies International. Available online: https://www.siemens.com/global/en/products/energy/grid-software/planning/pss-software/pss-e.html (accessed on 1 August 2022).
38. *IEEE Std 421.5-2016*; IEEE Recommended Practice for Excitation System Models for Power System Stability Studies. 2006. Available online: https://home.engineering.iastate.edu/~jdm/ee554/IEEEstd421.5-2016RecPracExSysModsPwrSysStabStudies.pdf (accessed on 25 August 2022).
39. IEEE PES Task Force, Dynamic Models for Turbine-Governors in Power System Studies, January 2013. Available online: https://resourcecenter.ieee-pes.org/publications/technical-reports/PESTR1.html (accessed on 30 December 2022).
40. Turbine-Governor Models, NEPLAN. 2015. Available online: https://www.neplan.ch/wp-content/uploads/2015/08/Nep_TURBINES_GOV.pdf (accessed on 1 January 2024).
41. Mugarra, A.; Guerrero, J.M.; Mahtani, K.; Platero, C.A. Synchronous Generator Stability Characterization for Gas Power Plants Using Load Rejection Tests. *Appl. Sci.* **2023**, *13*, 11168. [CrossRef]
42. Feltes, J.; Koritarov, V.; Guzowski, L.; Kazachkov, Y.; Lam, B.; Grande-Moran, C.; Thomann, G.; Eng, L.; Trouille, B.; Donalek, P. *Review of Existing Hydroelectric Turbine-Governor Simulation Models*; (No. ANL/DIS-13/05); Argonne National Lab (ANL): Argonne, IL, USA, 2013.
43. NERC, Modeling Notification Gas Turbine Governor Modeling, August 2017. Available online: https://www.nerc.com/comm/PC/NERCModelingNotifications/Gas_Turbine_Governor_Modeling.pdf (accessed on 5 September 2022).